공학박사 학위논문

MAC Layer Strategies for LTE-LAA Performance Enhancement

LTE-LAA 성능 향상을 위한 MAC 계층 기법

2019년 2월

서울대학교 대학원

전기·정보공학부

윤 강 진

공학박사 학위논문

MAC Layer Strategies for LTE-LAA Performance Enhancement

LTE-LAA 성능 향상을 위한 MAC 계층 기법

2019년 2월

서울대학교 대학원

전기·정보공학부

윤 강 진

MAC Layer Strategies for LTE-LAA Performance Enhancement

지도 교수 최 성 현

이 논문을 공학박사 학위논문으로 제출함

2019년 1월

서울대학교 대학원

전기·정보공학부

윤 강 진

윤강진의 공학박사 학위 논문을 인준함

2018년 12월

위 원 장: 박 세 웅 (인)

부위원장: 최 성 현 (인)

위 원: 임 종 한 (인)

위 원: 김 성 륜 (인)

위 원: 윤 지 훈 (인)

Abstract

3GPP long term evolution (LTE) operation in unlicensed spectrum is emerging as a promising technology in achieving higher data rate with LTE since ultra-wide unlicensed spectrum, e.g., about 500 MHz at 5–6 GHz range, is available in most countries. Recently, 3GPP has finalized standardization of licensed-assisted access (LAA) for LTE operation in 5 GHz unlicensed spectrum, which has been a playground only for Wi-Fi.

In this dissertation, we propose the following three strategies to enhance the performance of LAA: (1) Receiver-aware COT adaptation, (2) Collision-aware link adaptation, and (3) Power and energy detection threshold adaptation.

First, LAA has a fixed maximum channel occupancy time (MCOT), which is the maximum continuous transmission time after channel sensing, while Wi-Fi may transmit for much shorter time duration. As a result, when Wi-Fi coexists with LAA, Wi-Fi airtime and throughput can be much less than those achieved when Wi-Fi coexists with another Wi-Fi. To guarantee fair airtime and improve throughput of Wi-Fi, we propose a receiver-aware channel occupancy time (COT) adaptation (RACOTA) algorithm, which observes Wi-Fi aggregate MAC protocol data unit (A-MPDU) frames and matches LAA's COT to the duration of A-MPDU frames when any Wi-Fi receiver has more data to receive. Moreover, RACOTA detects saturation of Wi-Fi traffic and adjusts COT only if Wi-Fi traffic is saturated. We prototype saturation detection algorithm of RACOTA with commercial off-the-shelf Wi-Fi device and show that RACOTA detects saturation of Wi-Fi networks accurately. Through ns-3 simulations, we demonstrate that RACOTA provides airtime fairness between LAA and Wi-Fi while achieves up to 334% Wi-Fi throughput gain.

Second, the link adaptation scheme of the conventional LTE, *adaptive modulation and coding* (AMC), cannot operate well in the unlicensed band due to intermit-

tent collisions. Intermittent collisions make LAA eNB lower modulation and coding scheme (MCS) for the subsequent transmission and such unnecessarily lowered MCS significantly degrades spectral efficiency. To address this problem, we propose a collision-aware link adaptation algorithm (COALA). COALA exploits k-means unsupervised clustering algorithm to discriminate channel quality indicator (CQI) reports which are measured with collision interference and selects the most suitable MCS for the next transmission. By prototype-based experiments, we demonstrate that COALA detects collisions accurately, and by conducting ns-3 simulations in various scenarios, we also show that COALA achieves up to 74.9% higher user perceived throughput than AMC.

Finally, we propose PETAL to mitigate the negative impact of spatial reuse (SR) operation. We first design the baseline algorithm, which operates SR aggressively, and show that the baseline algorithm degrades the throughput performance severely when the UE is close to an interferer. Our proposed algorithm PETAL estimates and compares the spectral efficiency for the SR operation and non-SR operation. Then, PETAL operates SR only if the spectral efficiency of SR operation is expected to be higher than the case of non-SR operation. Our simulation verifies the performance of PETAL in various scenarios. When two pair of an eNB and a UE coexists, PETAL improves the throughput by up to 329% over the baseline algorithm.

In summary, we identify interesting problems that appeared with LAA and shows the impact of the problems through the extensive simulations and propose compelling algorithms to solve the problems. The airtime fairness between Wi-Fi and LAA is improved with COT adaptation. Furthermore, link adaptation accuracy and SR operation are improved by exploiting CQI reports history. The performance of the proposed schemes is verified by system level simulation.

keywords: Airtime fairness, licensed-assisted access (LAA), link adaptation, power control, spatial reuse (SR).

student number: 2012-20816

Contents

List of Tables

List of Figures

Chapter 1

Introduction

1.1 Motivation

With ever-increasing demand for wireless traffic, telecommunication firms and organizations are looking for solutions that can meet their needs. Recently, ITU-R has envisioned the future of mobile wireless technologies, where reaching a peak data rate of 20 Gb/s is considered one of the goals for the next generation wireless technology [1]. There are several approaches to improve peak data rate, e.g., utilizing higher order modulation and coding schemes, using more antennas, and exploiting wider frequency spectra. Recently, the 3rd generation partnership project (3GPP) has finished standardization of licensed-assisted access (LAA), which is a new feature introduced in 3GPP release 13, to support long-term evolution (LTE) downlink operation in 5 GHz unlicensed spectrum [2]. In many countries, there exist over 500 MHz unlicensed spectrum at 5 GHz. With LAA, LTE operators can use the rich unlicensed spectrum free of charge.

In this thesis, we focus on solving problems that occur when LTE-based technology (i.e., LAA) operates in the unlicensed band. LTE utilizes licensed band proprietarily and has no fairness issue with contending devices. On the other hand, LAA leverages 5 GHz unlicensed band which has been a playground for Wi-Fi. LAA de-

fines downlink transmission over 5 GHz spectrum, where channel sensing, i.e., listen before talk (LBT) operation similar to Wi-Fi medium access control (MAC) protocol, is performed before each transmission of eNodeB. LAA has a fixed maximum channel occupancy time (MCOT), which is the maximum continuous transmission time after channel sensing, while Wi-Fi may transmit for much shorter time duration. As a result, when Wi-Fi coexists with LAA, Wi-Fi airtime and throughput can be much less than those achieved when Wi-Fi coexists with another Wi-Fi.

Another problem is related to link adaptation. The link adaptation scheme of the conventional LTE, adaptive modulation and coding (AMC), cannot operate well in unlicensed band due to intermittent collisions. Intermittent collisions make LAA eNB lower modulation and coding scheme (MCS) for the subsequent transmission and such unnecessarily lowered MCS significantly degrades spectral efficiency.

The last problem of our interest is that the spatial reuse operation can degrade the spectral efficiency severely in some topologies. Simultaneous transmission with reduced power and increased energy detection threshold can improve the spectral efficiency if the interference from neighboring devices is not significant. However, if the UE is close to the interferer, the spatial reuse operation may bring significant spectral efficiency loss due to the degradation of signal quality.

1.2 Overview of Existing Approaches

1.3 Main Contributions

1.3.1 RACOTA: Receiver-Aware Channel Occupancy Time Adaptation for LTE-LAA

We propose a receiver-aware channel occupancy time (COT) adaptation (RACOTA) algorithm which observes Wi-Fi frames during channel sensing time and adjusts COT duration to the transmission duration of fully aggregated A-MPDU frames. Then, we

evaluate its performance in various aspects.

The main contributions of the chapter are as follows:

- We propose saturation detection (SD) algorithm which can detect fully aggregated A-MPDU frames without any information exchange between Wi-Fi transmitter and LAA enhanced node B (eNodeB). We implement SD algorithm in commercial off-the-shelf Wi-Fi devices[1] and evaluate its performance.
- We propose RACOTA, which detects Wi-Fi traffic saturation and adjusts maximum COT duration to the duration of an A-MPDU frame if Wi-Fi traffic is observed to be saturated.
- We evaluate the performance of RACOTA through extensive ns-3 simulations in various environments, including saturated traffic, unsaturated traffic, and bursty traffic. The Wi-Fi throughput gain of RACOTA over standard LAA is found to be up to 334%.

1.3.2 COALA: Collision-Aware Link Adaptation for LTE-LAA

We propose collision-aware link adaptation (COALA), a zero-overhead and standard-compliant link-adaptation scheme, capable of efficiently exploiting the transmission opportunities, especially, when there is intermittent interference caused by contention and/or hidden collisions. COALA achieves its goal by gauging optimal MCS with *CQI discrimination*. eNB discriminates the CQI reports, whose values are dominated by temporal interference (due to collision), and hence, unable to reflect the actual channel quality. We adopt k-means clustering algorithm to differentiate them, and accordingly, by using the result of the CQI discrimination, COALA selects the optimal MCS con-

[1] In reality, SD algorithm should be actually implemented inside LAA eNodeB, but we prototype SD algorithm with Wi-Fi device because LAA eNodeBs are not currently available. Being a passive algorithm, i.e., operating solely based on the reception of Wi-Fi frames, its performance can be validated even with the implementation with Wi-Fi device.

sidering whether the most recently received CQI is affected by collision interference as well as the estimated collision probability.

The main contributions of the chapter are as follows:

- We show that AMC, the default link-adaptation scheme of the conventional LTE, is not suitable for LAA in unlicensed band due to intermittent interference.
- We propose standard-compliant and zero-overhead link adaptation algorithm, COALA, which mitigates detrimental effect of intermittent interference on LAA's MCS selection.
- We implement the CQI clustering and collision detection algorithm of COALA on our USRP-based LAA testbed, and show its effectiveness through prototype-based experiments.
- We extensively evaluate the performance of COALA through ns-3 simulations.

1.3.3 PETAL: Power and Energy Detection Threshold Adaptation for LAA

We propose a power and energy detection threshold adaptation (PETAL) algorithm, a zero-overhead and standard-compliant power and energy detection threshold adaptation scheme, which utilizes CQI reports from UE. PETAL predicts and compares the spectral efficiency when the eNB performs SR and when it does not. PETAL performs SR only if the spectral efficiency of SR is expected to be higher than in the case of non-SR.

The main contributions of the chapter are as follows:

- We design a baseline algorithm which operates similar to OBSS-PD of IEEE 802.11ax and show that the baseline algorithm causes the throughput degradation when the UE is close to interferer.

- We propose a power and energy detection threshold adaptation algorithm, PETAL, which performs SR wisely and mitigates the deleterious effect of SR while the UE is likely to suffer from severe interference.
- We extensively evaluate the performance of PETAL through ns-3 simulations.

1.4 Organization of the Dissertation

The rest of the dissertation is organized as follows.

Chapter 2 presents RACOTA, a receiver-aware COT adaptation algorithm. First, we presents the related work and introduces basic medium access control (MAC) operation of Wi-Fi and LBT mechanism of LAA. Then, we discuss the unfairness between LAA and Wi-Fi and propose RACOTA algorithm. After that, SD algorithm of RACOTA is evaluated by measurement experiments and RACOTA is evaluated by simulation under various scenarios. Finally, we summarize the chapter with conclusion.

Chapter 3 presents COALA, a collision-aware link adaptation algorithm. First, we summarize background and related work and discuss the harmful impact of intermittent interference on AMC. Then, we propose COALA and demonstrate the feasibility and effectiveness of COALA via prototype-based experiments and ns-3 simulation, respectively. After that, we discuss several important points related to COALA. Finally, we summarize the chapter with conclusion.

Chapter 4 presents PETAL, a power and energy detection threshold adaptation algorithm. First, we summarize background and related work. Then we design a baseline algorithm which operates spatial reuse aggressively and show that the baseline algorithm degrades the throughput performance severely when the UE is close to an interferer. After that, we propose PETAL and evaluate the performance of PETAL via ns-3 simulation. Finally, we summarize the chapter with conclusion.

In Chapter 5, we conclude the dissertation with the summary of contributions and discussion on the future work.

Chapter 2

RACOTA: Receiver-Aware Channel Occupancy Time Adaptation for LTE-LAA

2.1 Introduction

With ever-increasing demand for wireless traffic, telecommunication firms and organizations are looking for solutions that can meet their needs. Recently, ITU-R has envisioned the future of mobile wireless technologies, where reaching a peak data rate of 20 Gb/s is considered one of the goals for the next generation wireless technology [1]. There are several approaches to improve peak data rate, e.g., utilizing higher order modulation and coding schemes, using more antennas, and exploiting wider frequency spectra.

Recently, the 3rd generation partnership project (3GPP) has finished standardization of licensed-assisted access (LAA), which is a new feature introduced in 3GPP release 13, to support LTE downlink operation in 5 GHz unlicensed spectrum [2]. In many countries, there exist over 500 MHz unlicensed spectrum at 5 GHz. With LAA, LTE operators can use the rich unlicensed spectrum free of charge. This is the most important driving force behind the advent of LAA. However, there are other wireless technologies, e.g., Wi-Fi, already operating at the same unlicensed band.

Thus, a spectrum-sharing mechanism is an essential function for LAA to act as a good neighbor, not an intruder to such incumbents. According to the LAA system design goal of 3GPP, LAA should provide fair coexistence with existing Wi-Fi networks by not degrading the Wi-Fi services more than an additional Wi-Fi network on the same carrier does with respect to throughput and latency [3].

Listen-before-talk (LBT) is a mechanism that requires the transmitter to apply a clear channel assessment (CCA) before using spectrum and transmit only if the spectrum is sensed to be idle. LAA is an LBT-based technology and its channel access procedure is similar to the enhanced distributed channel access (EDCA) of Wi-Fi. Once LAA has a chance to transmit, LAA can occupy a channel for up to maximum channel occupancy time (MCOT), while Wi-Fi occupies a channel during a physical (PHY) protocol data unit (PPDU) transmission time. Wi-Fi can use a frame aggregation function, called aggregate MAC protocol data unit (A-MPDU), to aggregate multiple MPDUs into one long PPDU to depreciate PHY/MAC protocol overhead. However, a PPDU transmission time can be limited to three factors: BlockAck bitmap size, maximum PHY service data unit (PSDU) length, and maximum PPDU duration. Our simulation results show that Wi-Fi coexisting with LAA and utilizing short PPDU transmission time may experience significant throughput degradation. This is because LAA occupies spectrum for 8 ms, while Wi-Fi takes a relatively short period of time for all transmission opportunities.

To address such airtime unfairness problem, we propose a receiver-aware channel occupancy time (COT) adaptation (RACOTA) algorithm which observes Wi-Fi frames during channel sensing time and adjusts COT duration to the transmission duration of fully aggregated A-MPDU frames. Then, we evaluate its performance in various aspects. Our main contributions are as follows:

- We propose saturation detection (SD) algorithm which can detect fully aggregated A-MPDU frames without any information exchange between Wi-Fi transmitter and LAA enhanced node B (eNodeB). We implement SD algorithm in commercial off-

the-shelf Wi-Fi devices[1] and evaluate its performance.

- We propose RACOTA, which detects Wi-Fi traffic saturation and adjusts maximum COT duration to the duration of an A-MPDU frame if Wi-Fi traffic is observed to be saturated.

- We evaluate the performance of RACOTA through extensive ns-3 simulations in various environments, including saturated traffic, unsaturated traffic, and bursty traffic. The Wi-Fi throughput gain of RACOTA over standard LAA is found to be up to 334%.

The remainder of the chapter is organized as follows. Section 2.2 presents the related work and Section 2.3 introduces basic medium access control (MAC) operation of Wi-Fi and LBT mechanism of LAA. The unfairness between LAA and Wi-Fi is discussed in Section 2.4 and we propose RACOTA algorithm in Section 2.5. Then, SD algorithm of RACOTA is evaluated by measurement experiments in Section 2.6 and RACOTA is evaluated by simulation under various scenarios in Section 2.7. Finally, the chapter is summarized in Section 2.8.

2.2 Related Work

The impact of LTE on Wi-Fi, when sharing the same unlicensed spectrum, has been studied in [4–6]. These papers show that when LTE and Wi-Fi coexist, total aggregate throughput is increased and LTE throughput is only slightly degraded, while Wi-Fi throughput is extremely hampered. Accordingly, they conclude that modifications to the LTE are needed in order to assure fair coexistence between LTE and Wi-Fi.

[1] In reality, SD algorithm should be actually implemented inside LAA eNodeB, but we prototype SD algorithm with Wi-Fi device because LAA eNodeBs are not currently available. Being a passive algorithm, i.e., operating solely based on the reception of Wi-Fi frames, its performance can be validated even with the implementation with Wi-Fi device.

As 5 GHz band offers a number of non-overlapping channels, employing a channel selection algorithm does alleviate the unfairness problem as discussed in [7]. With this solution, the overhead of deploying LTE in the unlicensed band is kept to a minimum. However, if Wi-Fi access points (APs) and LAA eNodeBs are densely deployed and there is no remaining contention-free channel, such a channel selection algorithm will fail to provide fairness. Thus, additional protocol to ensure fairness between LAA and Wi-Fi devices in a single channel is required.

To provide fairness in a single channel, various coexistence mechanisms have been proposed. Two most prominent methods are duty cycling and LBT. With the duty cycling approach, LTE transmitter is turned on and off with a predefined cycle. It transmits in the ON period and leaving the channel clear for Wi-Fi during the OFF period. The duration of the ON period is decided by channel sensing during the OFF period. In [8–12], the authors study the fairness between duty cycling LTE and Wi-Fi. In [13], Maglogiannis *et al.* propose a scheme which achieves proportional fairness between LTE-U and Wi-Fi networks by adjusting time duration of ON period and OFF period.

Another approach is the LBT [14–20]. Various modifications have been proposed to implement the LBT mechanism into LTE. The problem of using delayed ACKs to adaptively control contention window sizes is discussed in [14]. In [15], Jeon *et al.* discuss the effectiveness of LBT on outdoor and indoor deployments. Voicu *et al.* evaluate the effectiveness of LBT and channel selection in real world deployment in [16].

In [18–20], several coexistence methods, which adjust contention window value have been proposed. However, those methods cannot be used in countries whose regulation includes contention window doubling rule, e.g., EU [21]. Furthermore, they assume that LTE eNBs always can learn about coexisting Wi-Fi networks (for example, the throughput of Wi-Fi APs and the number of active Wi-Fi devices) and networks are always fully loaded. Such assumptions can hardly be achieved in a real environment.

In [22, 23], the effect of different COT values is discussed. They emphasize that

fairness between LAA and Wi-Fi can be severely damaged due to relatively short duration of Wi-Fi frames. However, they do not propose any algorithm that selects the optimal transmission time for fair coexistence.

In [24], Chai *et al.* address channel sensing asymmetry problem between Wi-Fi and unlicensed LTE. To solve this problem, they propose a solution which embeds Wi-Fi CTS-to-self frame in the OFDMA frame of unlicensed LTE.

2.3 MAC Mechanisms of Wi-Fi and LAA

2.3.1 Wi-Fi MAC Operation

Wi-Fi MAC follows carrier sense multiple access with collision avoidance (CSMA/CA) principle. When a Wi-Fi device has data to transmit, it performs carrier sensing. If the medium is assessed to be busy, the device defers transmission until the medium becomes idle. If the idle period is longer than arbitration interframe space (AIFS), which is 43 μs for best effort traffic, random backoff is performed. The backoff duration is set to *slot duration*, i.e., 9 μs, multiplied by a randomly selected *backoff counter* value.

There are multiple options that have been defined to manipulate the length of a Wi-Fi frame. When a frame delivered by upper layer is too long to accommodate, fragmentation can be applied to make it shorter. On the other hand, if a device intends to transmit a longer frame, it can use A-MPDU to aggregate multiple MPDUs into a single A-MPDU frame. A single A-MPDU transmission is restricted by the following limits. First, the maximum number of MPDUs in an A-MPDU frame is 64 due to the limitation of the BlockAck bitmap size. Second, PPDU transmission time should be less than or equal to a threshold (*PPDUMaxTime*), e.g., 10 ms and 5.484 ms for IEEE 802.11n and IEEE 802.11ac, respectively. Lastly, PSDU length of an A-MPDU frame cannot exceed a threshold (*PSDUMaxLength*), e.g., 65,535 bytes for IEEE 802.11n and 1,048,575 bytes for IEEE 802.11ac, respectively [25, 26].

A Wi-Fi station (STA) can obtain transmission opportunity (TXOP) time for its

consecutive frame transmission with the short interframe space (SIFS) spacing. During TXOP, a STA can transmit multiple frames which are in the same access category (AC) without additional backoff procedure. TXOPs for AC video (AC_VI) and AC voice (AC_VO) are 3.008 ms and 1.504 ms, respectively, which are relatively short compared to the 8 ms MCOT of LAA. Furthermore, AC background (AC_BK) and AC best effort (AC_BE) STAs are allowed to transmit only a single frame within a TXOP.

2.3.2 LAA Listen-Before-Talk (LBT) Mechanism

The design of LTE MAC is based on the orthogonal frequency division multiple access (OFDMA)-based physical layer and the characteristics of the radio resource occupancy; the radio resource is used in a time-slotted and frequency-divided manner. The radio resources at licensed spectrum are exclusively occupied by a certain operator. Therefore, an eNodeB can always control the usage of the radio and there is no contention required with eNodeBs of different operators as well as with the different types of technologies.

In LAA, however, the radio resource at unlicensed band is shared by neighboring LAA and Wi-Fi operating at the same frequency band, thus the LBT mechanism is needed. The main concept of LBT defined in LAA is similar to the channel access mechanism of Wi-Fi. LAA eNodeB should sense the channel and start transmission only if the channel is sensed to be idle during defer duration. The value of defer duration is 43 μs in case of channel access priority class 3, i.e., best effort traffic class, while the value can be different for other channel access priority classes. Even if the channel is sensed to be idle during defer duration, LAA eNodeB should wait until backoff counter becomes zero. Similar to Wi-Fi, backoff slot duration is set to 9 μs and backoff counter value is chosen randomly from zero to the contention window size. The contention window size is doubled whenever 80% of HARQ-ACK values of the starting subframe of the most recent transmission are determined as NACK [2].

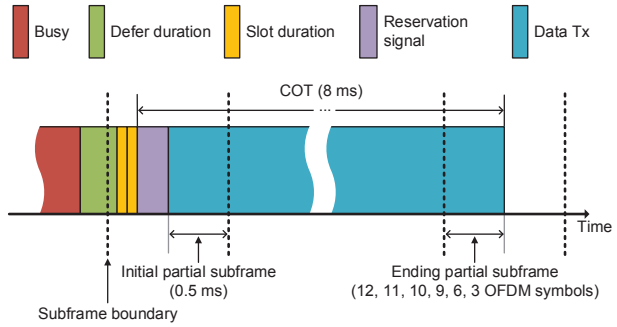

Figure 2.1: LBT mechanism of LAA.

Although the LBT mechanism of LAA is similar to that of Wi-Fi, there are several additional functional blocks defined in LAA to support its time-slotted and frequency-divided characteristics as illustrated in Fig. 2.1.

- Reservation signal: Since LAA eNodeB's channel access timing is not generally aligned with subframe boundaries, which appear every 1 ms, LAA eNodeB transmits a reservation signal before starting actual data transmission, which can normally occur at a subframe boundary. A reservation signal is a signal, sent without any information bits, such that other contending devices cannot grab the channel. In other words, ahead of data transmission, reservation signal transmission is needed, which is additional protocol overhead compared to the Wi-Fi channel access mechanism.

- Maximum channel occupancy time (MCOT): LAA eNB can transmit continuously up to MCOT. 3GPP has defined MCOT differently depending on the channel access priority class of data. MCOT is 2, 3, 8, and 8 ms for channel access priority classes 1, 2, 3, and 4, respectively. For priority classes 3 and 4, MCOT increases to 10 ms if the absence of other radio technologies that share wireless channel can be guaranteed. In addition to the data transmission time, the reservation signal transmission time should be included in MCOT. However, there are regulations about the time of continuous transmission in the unlicensed spectrum in some countries.

For example, EU and Japan have limited MCOT to 6 and 4 ms, respectively. In order for the LAA to be used in such countries, MCOT should be reduced to meet regulatory requirements.

- Partial subframe: To alleviate the reservation signal overhead, the partial subframe concept which allows partial usage of a subframe is introduced. There are two types of partial subframes, namely, initial partial subframe and ending partial subframe. Initial partial subframe (of 0.5 ms) enables LAA eNodeBs to start the transmission at the center of a subframe so that part of the reservation signal transmission is replaced by the data transmission. Ending partial subframe enables LAA eNodeBs to end the transmission in the middle of the subframe so that LAA eNodeBs make the most of COT duration. Ending partial subframe length can be chosen among 3, 6, 9, 10, 11, and 12 orthogonal frequency division multiplexing (OFDM) symbols, where a single full subframe is composed of 14 OFDM symbols. Utilizing both types of partial subframes may lengthen the data transmission time so that proportion of reservation signal may decrease, thus lowering the reservation signal overhead.

2.3.3 Wide Bandwidth Operation

Thanks to the channel bonding, Wi-Fi can leverage wide bandwidth. IEEE 802.11n supports 40 MHz operation while IEEE 802.11ac allows up to 160 MHz.

On the other hand, LTE supports carrier aggregation which has been standardized in 3GPP release 10. In 3GPP release 10, up to 5 component carriers and a total bandwidth of 100 MHz has been supported by carrier aggregation. However, a maximum number of component carriers and a total bandwidth has been increased to 32 and 640 MHz in 3GPP release 13.

Table 2.1: Simulation settings for Chapter 2 evaluation.

Simulation settings	Value
Simulation time	5 s
Number of iterations	10
File size	0.5 MB
Bandwidth	20, 40, 80 MHz
Wi-Fi PHY	802.11ac, 2×2 MIMO
Wi-Fi guard interval	800 ns
Wi-Fi maximum A-MPDU bound	5.484 ms, 1,048,575 bytes
Wi-Fi rate adaptation	Minstrel HT
AP/eNodeB transmission power	23 dBm
STA/UE transmission power	18 dBm
Wi-Fi CS/CCA threshold	−82 dBm
Wi-Fi CCA-ED threshold	−62 dBm
LAA CCA-ED threshold	−72 dBm

2.4 Coexistence performance of LAA and Wi-Fi

2.4.1 Simulation Setup

We have implemented an LAA and Wi-Fi coexistence model in *ns-3.22* [27], where LTE and Wi-Fi models are implemented in two separate and independent modules in the original version. In particular, interference between LAA and Wi-Fi, multiple input multiple out (MIMO) for LAA and Wi-Fi, 256 QAM and 80 MHz channel bonding operation, LTE carrier aggregation, LBT, LAA multiple carrier channel access procedure, 3GPP indoor hotspot channel model, and 3GPP file transfer protocol (FTP) traffic model [3] have been implemented. In 3GPP FTP model, 0.5 MB files arrive according to a Poisson process. LAA cannot use unlicensed spectrum without licensed spectrum, but we show LAA performance of unlicensed spectrum only for fair comparison with Wi-Fi; both LAA and Wi-Fi use the same 20, 40, and 80 MHz of unlicensed spectrum.

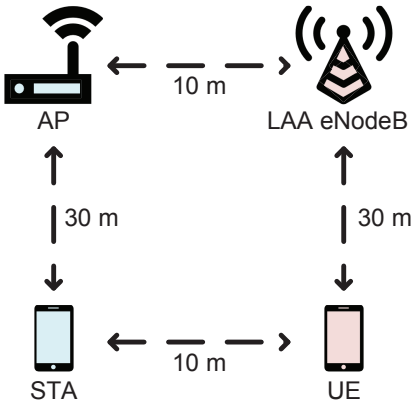

Figure 2.2: Simulation topology.

We assume that LTE control information is carried in licensed spectrum.

Simulation topology is illustrated in Fig. 2.2. There is one Wi-Fi access point (AP) transmitting data frames to a station (STA) and one LAA eNodeB transmitting data frames to a user equipment (UE) in the same unlicensed spectrum. In this chapter, we consider only downlink traffic, because 3GPP release 13 supports downlink LAA only. A Wi-Fi AP and an LAA eNodeB are 10 m apart from each other and the distance between the transmitter (i.e., AP or LAA eNodeB) and the receiver (i.e., STA or UE) is 30 m. There is a direct line-of-sight (LOS) path between all nodes [28]. In this topology, all nodes can observe each other, thus there is no hidden node. The detailed simulation settings are summarized in Table 3.1.

2.4.2 Unfairness between LAA and Wi-Fi

As we discussed in Section 2.3, LAA eNodeB accesses unlicensed spectrum using LBT mechanism similar to that of Wi-Fi. However, LAA eNodeB can occupy the channel for MCOT (e.g., 4, 6, 8 ms in Japan, EU, and US, respectively.), while Wi-Fi transmitter can occupy the channel only for one A-MPDU duration.

A Wi-Fi transmitter can aggregate multiple MPDUs into one A-MPDU frame within three limits: 1) Maximum number of MPDUs which is supported by Block-

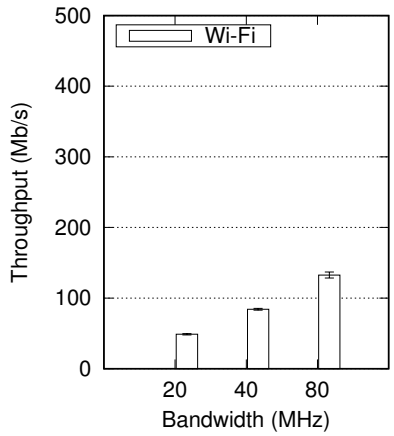

(a) Coexistence of two Wi-Fi APs.

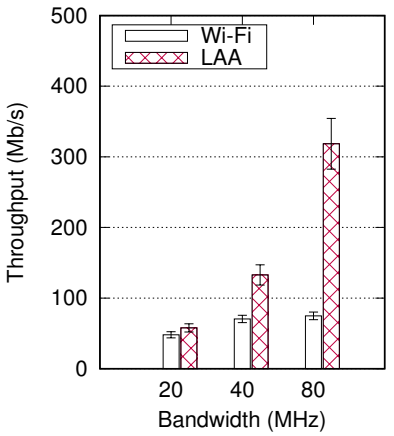

(b) Coexistence of Wi-Fi AP and LAA eNodeB in Japan (4 ms MCOT).

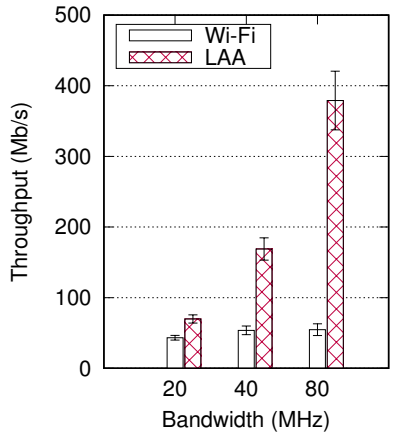

(c) Coexistence of Wi-Fi AP and LAA eNodeB in EU (6 ms MCOT).

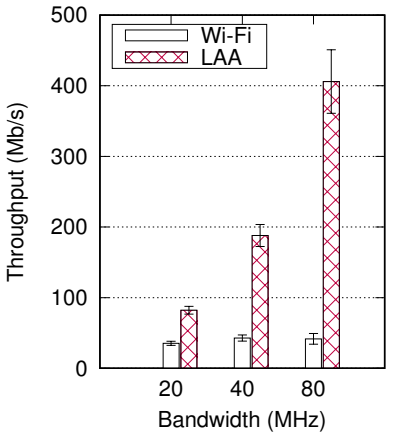

(d) Coexistence of Wi-Fi AP and LAA eNodeB in no MCOT regulation region (8 ms MCOT).

Figure 2.3: Throughput performance of various coexistence scenarios: Wide bandwidth degrades Wi-Fi throughput when Wi-Fi coexists with LAA.

Ack (64 MPDUs), 2) *PSDUMaxLength* (1,048,575 bytes), and 3) *PPDUMaxTime*. IEEE 802.11ac specification defines *PPDUMaxTime* as 5.484 ms, but *PPDUMaxTime* should be shorter than 4 ms in Japan. Even if the *PPDUMaxTime* value of Wi-Fi trans-

mitter is set to 5.484 ms, the duration of the aggregated A-MPDU frame can be short when the Wi-Fi transmitter uses high data rate and its MPDU aggregation is limited by the BlockAck bitmap size or *PSDUMaxLength* bound. IEEE 802.11ac devices can use high data rate thanks to 256-QAM and wide channel bonding (up to 160 MHz). Accordingly, the duration of A-MPDU frame of the 11ac device is likely to be shorter than *PPDUMaxTime*.

Therefore, fixed MCOT value of LAA can cause a severe airtime unfairness problem especially when Wi-Fi A-MPDU duration is relatively short. Wi-Fi A-MPDU duration can be less than MCOT when the value of *PPDUMaxTime* is below MCOT or Wi-Fi transmission rate is high enough to transmit *PSDUMaxLength* $(1,048,575$ bytes) or 64 MPDUs within MCOT. In this sense, we claim that standard LAA is not a good neighbor to Wi-Fi in some coexistence scenarios.

Fig. 2.3a shows throughput performance when two Wi-Fi APs coexist, while Figs. 2.3b, 2.3c, and 2.3d show throughput performance when an LAA eNodeB coexists with a Wi-Fi AP in Japan, EU, and US, respectively. In Fig. 2.3, we observe that the throughput of Wi-Fi is degraded more severely as the bandwidth of Wi-Fi becomes broader. Increased Wi-Fi data rate due to broader bandwidth results in shorter A-MPDU duration, while LAA does not change MCOT based on the number of aggregated carriers. The problem is exacerbated as MCOT of LAA increases. In Fig. 2.3d, we observe that the throughput of Wi-Fi is worse than that of Wi-Fi in a coexistence case of two Wi-Fi APs (Fig. 2.3a) even with the 20 MHz.

2.5 Receiver-Aware COT Adaptation Algorithm

In this section, we propose RACOTA to improve airtime fairness between LAA and Wi-Fi. The core idea of RACOTA is that LAA's COT should not be longer than A-MPDU transmission duration of coexisting Wi-Fi network for fair coexistence. However, short COT can cause more frequent transmission of reservation signals and bring

Algorithm 1 Saturation detection algorithm

Input: Wi-Fi frame observation

T_{longest}: Longest PPDU duration
$T_{\mathrm{resetLongest}}$: Reset interval of T_{longest}
C: Number of consecutive frames which are most probably bounded by T_{longest}
C_{thres}: Threshold for *PPDUMaxTime* detection
D: Whether T_{longest} is detected to be *PPDUMaxTime*
S: Saturation indicator (i.e., whether A-MPDU frame is fully aggregated or not)

loop
    Reset T_{longest} every $T_{\mathrm{resetLongest}}$ seconds
    if Observed Wi-Fi frame is an A-MPDU frame **then**
        $S \leftarrow false$
        $M \leftarrow$ Number of MPDUs in the A-MPDU frame
        $L \leftarrow$ Length of the A-MPDU frame
        $L_{\mathrm{mpdu}} \leftarrow$ Average length of MPDUs in the A-MPDU frame
        $T \leftarrow$ PPDU duration of the A-MPDU frame
        $R \leftarrow$ Data rate of the A-MPDU frame
        $T_{\mathrm{mpdu}} \leftarrow$ Average duration of MPDUs in the A-MPDU frame (L_{mpdu}/R)
        $A \leftarrow$ Receiver MAC address of the A-MPDU frame
        if $M = 64$ or $L \geq$ *PSDUMaxLength*$-L_{\mathrm{mpdu}}$ **then**
            $S \leftarrow true$
        else
            if $T > T_{\mathrm{longest}}$ **then**
                $T_{\mathrm{longest}} \leftarrow T$; $C \leftarrow 1$
            else if $C \neq 0$ **then**
                if $T \geq T_{\mathrm{longest}} - T_{\mathrm{mpdu}}$ **then**
                    $C \leftarrow C + 1$
                else
                    $D \leftarrow false$; $C \leftarrow 0$
                end if
            else
                if $T \geq T_{\mathrm{longest}} - T_{\mathrm{mpdu}}$ **then**
                    $C \leftarrow 1$
                end if
            end if
            if $C > C_{\mathrm{thres}}$ **then**
                $D \leftarrow true$; $C \leftarrow 0$
            end if
        end if
        if $D = true$ and $T > T_{\mathrm{longest}} - T_{\mathrm{mpdu}}$ **then**
            $S \leftarrow true$
        end if
    else if Observed non A-MPDU frame is not a control or management frame **then**
        if $C \neq 0$ **then**
            $D \leftarrow false$; $C \leftarrow 0$
        end if
    end if
    return A, S, T
end loop

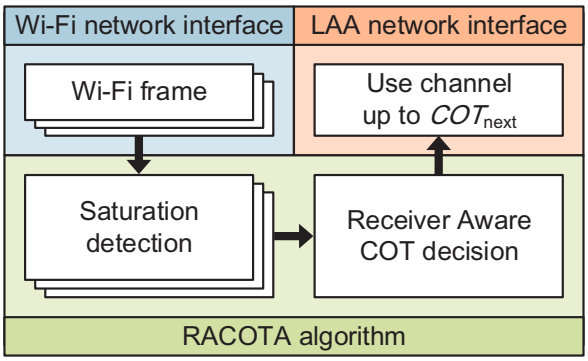

Figure 2.4: Flow chart of RACOTA.

more protocol overhead. Therefore, RACOTA adapts its COT only if an A-MPDU frame to any coexisting Wi-Fi receiver is fully aggregated because it means that the Wi-Fi receiver has more data to receive even after receiving this A-MPDU frame and its corresponding Wi-Fi transmitter needs more time to send them. In this situation, the Wi-Fi network is said to be "saturated."

The basic strategy of RACOTA is divided into two steps:

1. Saturation detection (SD): RACOTA runs SD algorithm to figure out whether coexisting Wi-Fi networks are saturated or not. For this purpose, we assume that an LAA eNodeB overhears Wi-Fi frames by the aid of a Wi-Fi module co-located with eNodeB.[2]

2. Receiver-aware COT decision: RACOTA adapts COT to the longest transmission duration among the saturated Wi-Fi networks. RACOTA resets COT to the duration of MCOT (T_{MCOT}) if no Wi-Fi network is saturated.

[2]This could bring extra cost, but considering the advantage of using Wi-Fi module in LAA eNodeBs, many LAA eNodeBs are expected to include Wi-Fi module in practice. For example, Broadcom recently applied for a patent in which they assume to embed a Wi-Fi AP in an unlicensed LTE eNodeB [29].

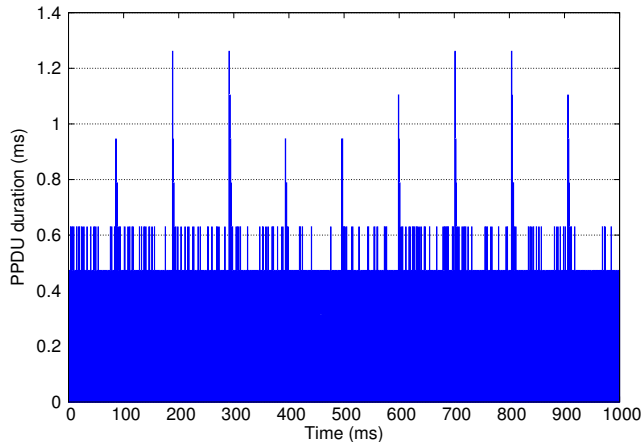

Figure 2.5: PPDU duration measurement result in a clean channel.

2.5.1 Saturation Detection (SD)

A Wi-Fi network is considered saturated if an observed A-MPDU frame satisfies one of the following criteria:

1. A-MPDU consists of maximum number of MPDUs (M) which is equal to the BlockAck bitmap size, i.e., 64.

2. PSDU length of the A-MPDU frame (L) is greater than or equal to *PSDUMaxLength*$-L_{\mathrm{mpdu}}$, where L_{mpdu} is the average length of MPDUs in the A-MPDU frame.

3. PPDU duration of the A-MPDU frame (T) is greater than or equal to *PPDUMaxTime*$-T_{\mathrm{mpdu}}$, where *PPDUMaxTime* is the maximum PPDU duration, and T_{mpdu} is the average duration of MPDUs in the A-MPDU frame. T_{mpdu} can be calculated by dividing L_{mpdu} by the data rate of the A-MPDU frame (R).

PPDUMaxTime can differ by Wi-Fi NIC settings while the BlockAck bitmap size and $PSDUMaxLength$ should be the same for all Wi-Fi NIC settings. To check the third condition, SD algorithm continues to track the *PPDUMaxTime* of each Wi-Fi transmitter.

SD algorithm maintains the longest PPDU duration of each Wi-Fi transmitter and infers whether their transmission is bounded by *PPDUMaxTime*. If the transmission duration of a Wi-Fi transmitter is always the same, SD algorithm does not have any clue to infer. Constant bitrate (CBR) traffic with source rate under the Wi-Fi transmitter's achievable throughput may be the case. However, even in this case, A-MPDU transmission duration is not consistent for the following reasons:

1. Other devices' intermittent channel occupancy: Even if a Wi-Fi transmitter has CBR traffic, the number of frames in the transmission queue of the Wi-Fi transmitter can increase drastically when other devices transmit their signals sporadically. Accordingly, an A-MPDU frame, which is transmitted right after other device's transmission, is likely to convey more MPDUs than usual.

2. Beacon transmission: Wi-Fi beacon frames are transmitted periodically by Wi-Fi AP with a period of 102.4 ms typically. During the time duration of beacon transmission, more frames may arrive at transmission queue and Wi-Fi transmitter may transmit longer A-MPDU frame than usual.

Fig. 2.5 shows PPDU duration measurement results when Wi-Fi transmitter has CBR traffic of 50 Mb/s and fixed PHY rate of 78 Mb/s. The experiment is conducted in a clean 5 GHz channel, meaning that there are no other nearby radio transmitters. Even though there is no contending signal, the PPDU duration of A-MPDU frames increases dramatically once every 102.4 ms due to beacon signals.

SD algorithm updates T_{longest} when it observes A-MPDU frame longer than current T_{longest}, and checks the subsequent A-MPDU frames if they are restricted by *PPDUMaxTime*. If the observed T_{longest} is caused by channel occupancy of contending devices' intermittent traffic or Wi-Fi beacon frame, T of the subsequent A-MPDU frames may decrease dramatically. On the other hand, if the observed T_{longest} is PPDU duration which is restricted by *PPDUMaxTime*, T of the subsequent A-MPDU frames may have similar transmission time until there are not enough frames in the transmis-

sion queue. If SD algorithm observes A-MPDU frames whose transmission time is greater than or equal to $T_{\text{longest}} - T_{\text{mpdu}}$ consecutively more than C_{thres} times, SD algorithm concludes that T_{longest} is *PPDUMaxTime*. However, if the number of consecutive A-MPDU frames with similar transmission duration is smaller than C_{thres}, SD algorithm concludes that *PPDUMaxTime* is not detected yet, and do not use *PPDUMaxTime* bound for saturation detection.

Finally, the saturation detection results, i.e., receiver MAC address (A), saturation indicator (S), PPDU duration of the A-MPDU frame (T) is passed to the next algorithm's input. The pseudo-code of SD algorithm is presented in Algorithm 1.

2.5.2 Receiver-Aware COT Decision

As presented in Algorithm 2, RACOTA manages the outcome of SD algorithm (Algorithm 1), namely, saturation indicator (S_i), PPDU duration (T_i), and MAC address A_i, for each Wi-Fi receiver i. RACOTA updates them whenever SD algorithm returns the information, or resets them if no frame is detected for Wi-Fi receiver i during T_{reset}. RACOTA adjusts next COT duration (COT_{next}) to the maximum T_i among saturated Wi-Fi receivers (meaning $S_i = true$) with an upper bound of T_{MCOT}, while RACOTA uses the default COT duration of T_{MCOT} if every Wi-Fi receiver is unsaturated, i.e., every receiver has no more data to receive. The reason why RACOTA judges based on the Wi-Fi receiver rather than the transmitter is that same problem may happen when a single Wi-Fi transmitter has heterogeneous traffic to multiple receivers.

2.6 Performance Evaluation of SD Algorithm

2.6.1 Measurement Setup

We have implemented Wi-Fi frame observation and SD algorithm parts of RACOTA in a commercial off-the-shelf 802.11n device, Qualcomm Atheros AR9380 NIC, by modifying the open-source device driver *ath9k* [30]. *hostAP* [31] daemon program is

Algorithm 2 Receiver-aware channel occupancy time decision algorithm

Input: S_i, T_i for $i = 1, \cdots, N$

T_{MCOT} : Time duration of MCOT

T_{reset}: Reset interval of S, T

N: Total number of observed Wi-Fi receivers

S_i: S of ith observed Wi-Fi receiver

T_i: T of ith observed Wi-Fi receiver

loop

    Reset S_i, T_i to 0, if no frame to Wi-Fi receiver i is observed during T_{reset}

    $COT_{\text{next}} \leftarrow 0$ ms

    for $i = 1, \cdots, N$ **do**

        if $S_i = true$ **then**

            $COT_{\text{next}} \leftarrow \max(COT_{\text{next}}, T_i)$

        end if

    end for

    if $\sum_{i=1}^{N} S_i = false$ **then**

        $COT_{\text{next}} \leftarrow T_{MCOT}$

    else

        $COT_{\text{next}} \leftarrow \min(COT_{\text{next}}, T_{MCOT})$

    end ifreturn COT_{next}

end loop

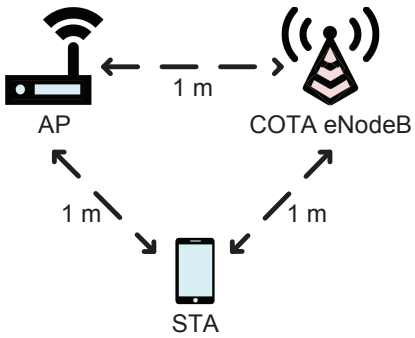

Figure 2.6: Measurement topology for SD algorithm validation.

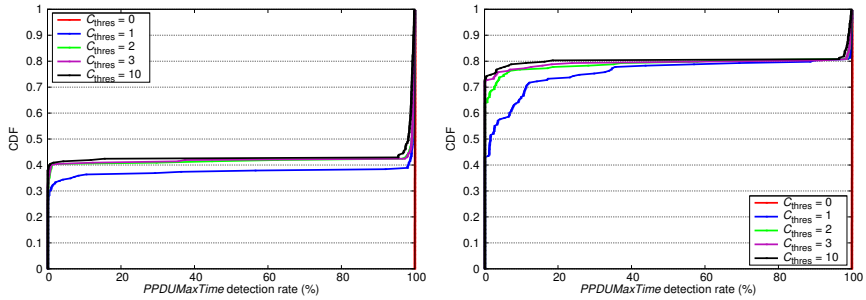

(a) 60 Mb/s source rate.

(b) 20 Mb/s source rate.

Figure 2.7: Impact of C_{thres} on *PPDUMaxTime* detection rate.

used to build an AP on Ubuntu 14.04 machine and *Iperf* 2.0.5 [32] is used to generate Wi-Fi UDP traffic. We have conducted our experiments in an office environment with a 20 MHz operating channel (channel number 153 with 5.765 GHz center frequency) which has no interference signal. Fig. 2.6 illustrates the topology of our measurement experiments. We place nodes 1 m apart from each other and install an Ubuntu machine implementing SD instead of RACOTA eNodeB. There is no uplink traffic and MPDU size is fixed to 1,538 bytes.

2.6.2 *PPDUMaxTime* Detection

Fig. 2.7 shows the empirical cumulative distribution function (CDF) of *PPDUMaxTime* detection rate of various C_{thres} values. *PPDUMaxTime* detection rate is defined as the number of A-MPDU frames whose T_{longest} is detected to be *PPDUMaxTime* over the total number of A-MDPU frames. Every combination of eleven PHY rates (13, 19.5, 26, 39, 52, 58.5, 65, 78, 104, 117, 130 Mb/s) and nine *PPDUMaxTime* values (2, 3, 4, 5, 6, 7, 8, 9, 10 ms) (total 99 combinations) are tested in two different CBR traffic environments, i.e., 60 Mb/s and 20 Mb/s. If source rate is greater than achievable throughput, which is determined by PHY rate and *PPDUMaxTime* value, A-MPDU frames will be fully aggregated. If SD algorithm observes fully-aggregated A-MPDU frames, which have transmission time greater than or equal to $T_{\mathrm{longest}} - T_{\mathrm{mpdu}}$, con-

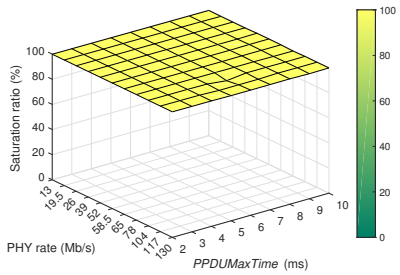

(a) Saturated Wi-Fi traffic environment.

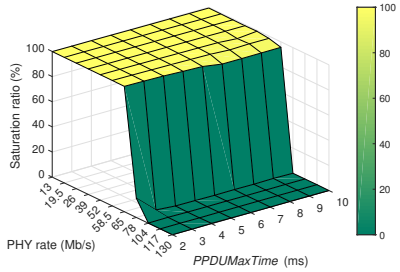

(b) 60 Mb/s Wi-Fi CBR traffic environment.

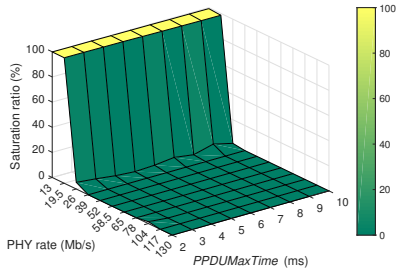

(c) 20 Mb/s Wi-Fi CBR traffic environment.

Figure 2.8: Saturation detection performance of RACOTA.

secutively more than C_{thres} times, it concludes that *PPDUMaxTime* has been detected. However, if C_{thres} value is too small, SD algorithm can misconceive the PPDU duration of not fully aggregated A-MPDU frame as *PPDUMaxTime*.

In Figs. 2.7a and 2.7b, we observe that *PPDUMaxTime* detection rate is almost 100% when C_{thres} is set to 0. This is because SD algorithm identifies T_{longest} as *PPDUMaxTime* without any consecutive observation if C_{thres} is set to 0. On the other

hand, SD algorithm detects *PPDUMaxTime* more sharply as C_{thres} increases. A-MPDU frames are limited by *PPDUMaxTime* and *PPDUMaxTime* should be detected in sixty combinations ($60/99 \simeq 0.6$) and eighteen combinations ($18/99 \simeq 0.2$) for 60 Mb/s source rate case and 20 Mb/s source rate case, respectively. When C_{thres} is greater than 1, CDF curves show clear discrimination performance of SD. We assume $C_{\mathrm{thres}} = 3$ for the rest of the chapter.

2.6.3 Saturation Detection Performance

We evaluate saturation detection performance of RACOTA with various Wi-Fi traffic source rates. Fig. 2.8a shows saturation detection performance of RACOTA with saturated Wi-Fi traffic. To generate saturated Wi-Fi traffic, *Iperf* source rate is set to 500 Mb/s CBR traffic. Because even our highest PHY rate (130 Mb/s) is lower than this CBR source rate, Wi-Fi transmission queue is always occupied by a myriad of frames and Wi-Fi transmitter aggregates its MPDUs until when it exceeds one of aforementioned aggregation limits.

We define saturation ratio as the number of A-MPDU frames, which SD algorithm detects saturation, over the total number of observed A-MPDU frames. Saturation ratio is almost 100% for any PHY rate and *PPDUMaxTime*. Lower PHY rate makes longer MPDU transmission time and A-MPDU frames can be limited by *PPDUMaxTime*. On the other hand, higher PHY rate shortens its MPDU transmission time, and hence, A-MPDU frames can be easily limited by BlockAck bitmap size or *PSDUMaxLength*. At low PHY rate, SD algorithm detects Wi-Fi transmitters' *PPDUMaxTime* and compares the PPDU duration of observed A-MPDU frames and returns its saturation information. On the other hand, SD algorithm compares the number of MPDUs in A-MPDU frames with BlockAck bitmap size and PSDU size of A-MPDU frames with *PSDUMaxLength*. Fig. 2.8a shows that saturation detection ratio of SD algorithm is almost 100% for all PHY rates and *PPDUMaxTime*'s.

Figs. 2.8b and 2.8c present detection performance when Wi-Fi CBR traffic is set to 60 Mb/s and 20 Mb/s, respectively. Depending on what Wi-Fi PHY rates and *PPDUMaxTime* are used, this CBR traffic could be saturated traffic or unsaturated traffic. In Figs. 2.8b and 2.8c, we can observe that SD algorithm successfully detects saturation when PHY rate is lower than source rates (60 Mb/s or 20 Mb/s) and detects non-saturation when PHY rate is much higher than source rates.

2.7 Performance Evaluation

In this section, we evaluate the performance of RACOTA under various simulation scenarios. We consider three different traffic scenarios: Saturated traffic, unsaturated traffic, and bursty traffic. LAA MCOT can be different according to channel access priority class and MCOT should be less than maximum continuous transmission time regulation in some countries. However, we only consider the priority class 3 traffic (best effort traffic) and countries which have no continuous transmission time regulation (e.g., U.S. and Korea) for the rest of the chapter ($T_{MCOT} = 8$ ms). Note that the overall trends should remain the same irrespective of the traffic class and MCOT regulation.

The following five coexistence cases are evaluated in this section:

- Wi-Fi+Wi-Fi: Wi-Fi and Wi-Fi coexist.
- Wi-Fi+RACOTA: Wi-Fi and LAA adopting RACOTA coexist.
- Wi-Fi+LAA: Wi-Fi and standard LAA coexist.
- Wi-Fi+COTA: Wi-Fi and COT adaptation (COTA) [33] algorithm coexist.

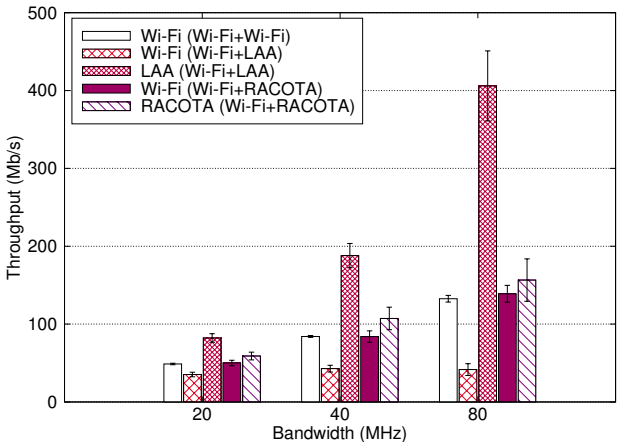

Figure 2.9: Throughput performance of RACOTA.

2.7.1 Saturated Traffic Scenario

Throughput Performance

Fig. 2.9 shows the throughput performance of coexisting devices with 20, 40, and 80 MHz bandwidth. In Wi-Fi+LAA, Wi-Fi throughput is getting worse than that of Wi-Fi+Wi-Fi as the bandwidth gets wider, which shows the same tendency discussed in Section 2.4. In Wi-Fi+RACOTA, the Wi-Fi throughput increases and its value is almost the same as that of Wi-Fi+Wi-Fi, since RACOTA matches the COT to the sensed A-MPDU duration when it determines that neighboring Wi-Fi network is saturated. Accordingly, Wi-Fi occupies more airtime and its throughput increases, while LAA throughput decreases. As explained above, RACOTA cares the Wi-Fi network by yielding its exclusively occupied airtime.

Airtime Fairness

Fig. 2.10a shows fractional airtime ratio results. We define fractional airtime ratio as total transmission time over the total simulation time. If Wi-Fi coexists with standard LAA, fractional airtime ratio of standard LAA increases as Wi-Fi bandwidth get wider, due to the fixed 8 ms COT value of standard LAA. In Fig. 2.10a, we observe that

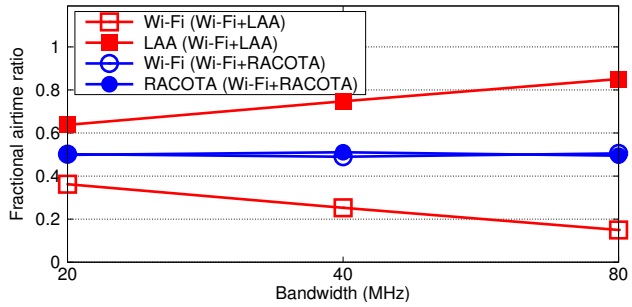

(a) Fractional airtime ratio.

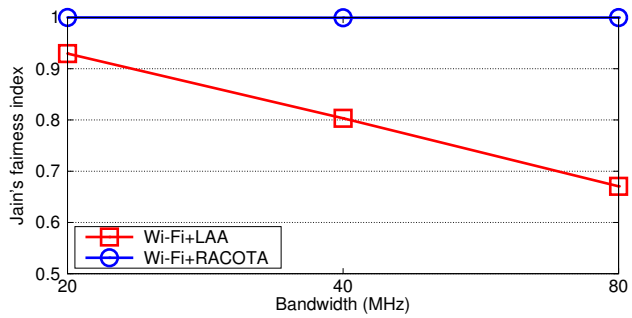

(b) Jain's fairness index.

Figure 2.10: Airtime fairness of RACOTA.

standard LAA occupies about 5.7 times more airtime than Wi-Fi when Wi-Fi and LAA use 80 MHz bandwidth. On the other hand, RACOTA guarantees almost half the airtime to Wi-Fi regardless of its A-MPDU duration.

We use Jain's fairness index to compare airtime fairness between Wi-Fi+LAA and Wi-Fi+RACOTA. The definition of Jain's fairness index is as follows:

$$J(x_1, x_2, \cdots, x_n) = \frac{(\sum_{i=1}^{n} x_i)^2}{n \sum_{i=1}^{n} x_i^2}.$$

The fairness index ranges from $1/n$ (the worst case) to 1 (the best case), achieving the maximum when all users receive the same allocation. Fig. 2.10b shows that the fairness index is very close to 1 when RACOTA is adopted while the fairness index is much lower when standard LAA is used.

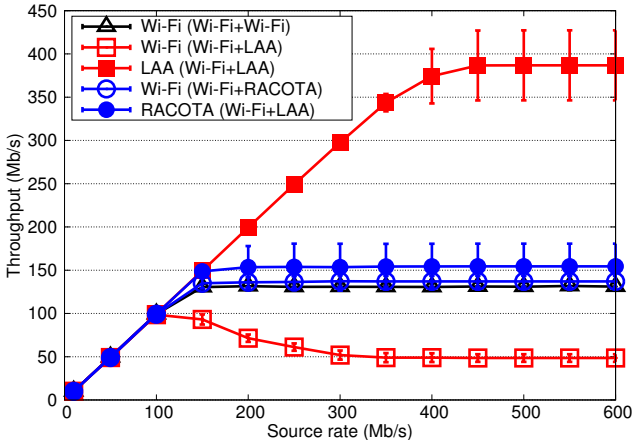

Figure 2.11: Unsaturated traffic scenario.

2.7.2 Unsaturated Traffic Scenario

We investigate how RACOTA operates with unsaturated traffic. Fig. 2.11 presents the throughput results of Wi-Fi+Wi-Fi, Wi-Fi+LAA, and Wi-Fi+RACOTA with various source rates. To achieve various source rates (10–600 Mb/s), we reduce file size to 12.5 KB and vary file arrival rate (100–6,000 files/s). We use the same topology as saturated Wi-Fi traffic simulations, but utilize 80 MHz bandwidth only. In Fig. 2.11, we can observe that RACOTA and standard LAA show the similar behavior when source rate is less than 100 Mb/s, because RACOTA adapts COT only if Wi-Fi has saturated traffic. On the other hand, RACOTA outperforms standard LAA in terms of Wi-Fi throughput thanks to the capability of COT adaptation when the network is saturated.

2.7.3 Bursty Traffic Scenario

Figs. 2.12a and 2.12b illustrate behavior of RACOTA in case of bursty Wi-Fi traffic scenario. To simulate such scenario, we increase Wi-Fi file size to 1.25 MB and reduce Wi-Fi file arrival rate to 0.5 files/s (i.e., 5 Mb/s Wi-Fi source rate). Wi-Fi file arrivals are illustrated as black vertical lines in Figs. 2.12a and 2.12b. As we can

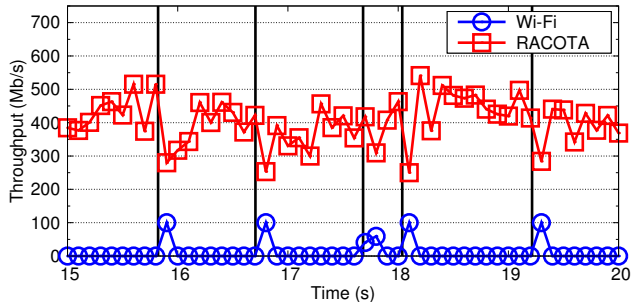

(a) Instantaneous throughput trace.

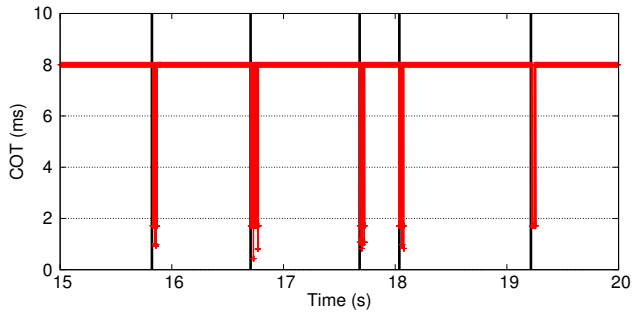

(b) COT trace.

Figure 2.12: Bursty Wi-Fi traffic scenario.

observe in Fig. 2.12a, Wi-Fi throughput increases when files arrive and Wi-Fi transmitters start to send data and decreases to 0 Mb/s when file transmissions have been finished. Throughput performance of LAA, which utilizes RACOTA, decreases during Wi-Fi file transmission time and increases when the Wi-Fi file transmission is finished. Fig. 2.12b shows that RACOTA shortens COT immediately to the duration of A-MPDU frames and restores COT to the default duration of T_{MCOT} when Wi-Fi finishes its file transmission.

2.7.4 Heterogeneous Wi-Fi Traffic Generation Scenario

Our prior work, COTA [33], adapts COT duration based on A-MPDU statistics which are observed since the latest LAA transmission. Therefore, COTA may not adapt its COT duration properly in complicated situations. Fig. 2.13 shows an example topol-

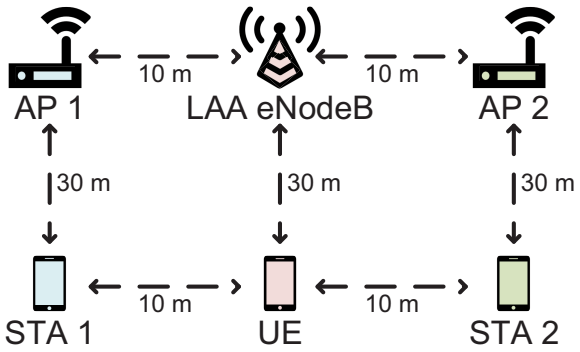

Figure 2.13: Simulation topology of the heterogeneous Wi-Fi traffic generation scenario.

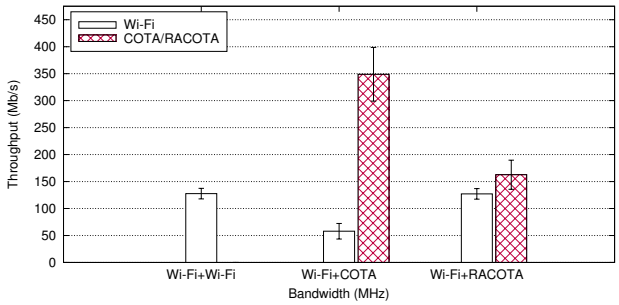

Figure 2.14: Impact of the heterogeneous Wi-Fi traffic generation on COTA and RACOTA.

ogy in which COTA may not operate fairly with Wi-Fi networks. Provided that AP 1 has unsaturated traffic while AP 2 has saturated traffic, COTA may not observe traffic from AP 2 during sensing time. As a result, COTA ends up using T_{MCOT} COT duration instead of adjusting COT duration so that fair airtime for Wi-Fi networks is not guaranteed.

RACOTA solves this problem by managing saturation indicator (S_i) value and the PPDU duration (T_i) value for every nearby Wi-Fi receiver i. RACOTA adjusts COT duration if at least one S_i is true, meaning that there is at least one Wi-Fi receiver whose last transmission of A-MPDU is considered saturated. The largest value among

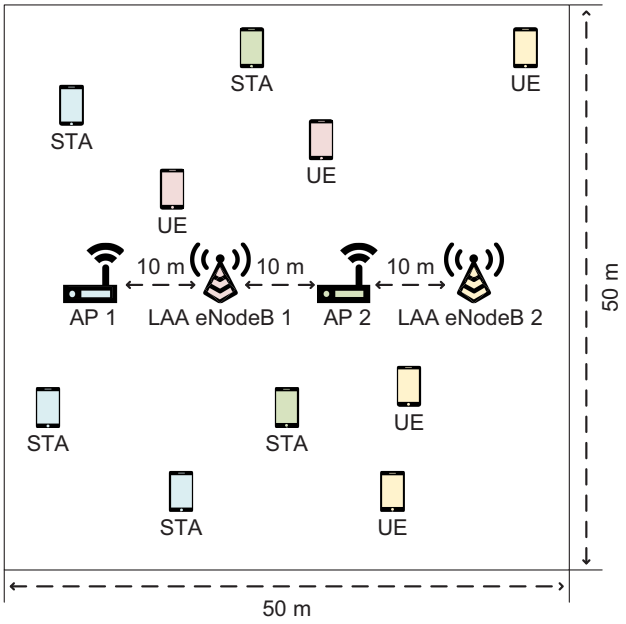

Figure 2.15: Example of multiple node simulation topology.

T_i of saturated Wi-Fi receivers is selected for COT_{next}. In Fig. 2.13, even if RACOTA does not observe traffic from AP 2, RACOTA can use valid historical information of AP 1 to correctly determine whether COT duration should be adjusted.

In this scenario, AP 1 has intermittent unsaturated traffic (generating 200 files of 3.125 KB per second) and AP 2 has saturated traffic, while both APs utilize same 80 MHz bandwidth. RACOTA reduces COT to the time duration of fully aggregated A-MPDU frame for almost every transmission. The throughput results in Fig. 2.14 show that if a Wi-Fi network coexists with RACOTA, it can achieve throughput performance as much as when a Wi-Fi network coexists with another Wi-Fi network. However, COTA's wrong COT decision raises an airtime unfairness problem, thus decreasing Wi-Fi throughput.

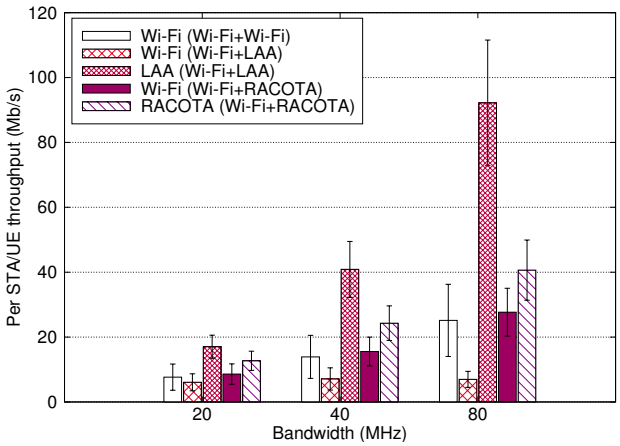

Figure 2.16: Multiple node scenario: Two Wi-Fi APs, five Wi-Fi STAs, two LAA eNodeBs, and five LAA UEs.

2.7.5 Multiple Node Scenario

We evaluate the performance of RACOTA in a multiple node scenario. Fig. 2.15 shows an example of multiple node topology in consideration. Two Wi-Fi APs and two LAA eNodeBs coexist in a 50×50 m^2 room, where the distance between each AP and eNodeB is 10 m. STAs and UEs are randomly placed and connected to an AP or an eNodeB of which signal is the strongest signal. LAA eNodeBs and UEs are replaced by Wi-Fi APs and STAs in the Wi-Fi+Wi-Fi scenario.

Fig. 2.16 shows per-STA/UE throughput performance when four base stations (APs or eNodeBs) and ten user devices (STAs or UEs) coexist. In Wi-Fi+RACOTA, per-STA Wi-Fi throughput is almost the same as that of Wi-Fi+Wi-Fi, thanks to RACOTA's COT adaptation. On the other hand, in Wi-Fi+LAA, per-STA Wi-Fi throughput is far smaller than that of Wi-Fi+Wi-Fi, especially when wide bandwidth is used. When Wi-Fi coexists with RACOTA, its throughput improves by up to 297% (when 80 MHz bandwidth is used) compared to the case when Wi-Fi coexists with standard LAA. We observe that RACOTA successfully adjusts LAA COT so that LAA does not degrade throughput performance of coexisting Wi-Fi network more than an additional Wi-Fi

network even in complex topology.

2.8 Summary

In this chapter, we propose a COT adaptation algorithm for LAA to be a more friendly neighbor to Wi-Fi. We first show that LAA can degrade the performance of Wi-Fi via ns-3 simulation. This is because LAA uses fixed MCOT regardless of Wi-Fi frame duration, and tends to occupy more airtime than Wi-Fi. To solve this problem, we propose RACOTA, a COT adaptation algorithm, which adjusts COT to the duration of a fully aggregated A-MPDU frame. We implement saturation detection algorithm of RACOTA in commercial off-the-shelf Wi-Fi NIC and measurement results demonstrate that RACOTA can detect saturation of Wi-Fi networks successfully. Simulation results show that in the case when Wi-Fi coexists with RACOTA, Wi-Fi can occupy about half the airtime and its throughput improves by up to 334% compared to the case when Wi-Fi coexists with standard LAA. Furthermore, the simulation results in various scenarios show that RACOTA can detect saturation of Wi-Fi traffic successfully and adjust COT only if Wi-Fi traffic is saturated. Simulations with the heterogeneous Wi-Fi traffic generation scenario and in multiple node environments show that RACOTA can properly adjust COT in a real-world environment.

Chapter 3

COALA: Collision-Aware Link Adaptation for LTE-LAA

3.1 Introduction

Leveraging unlicensed band for long-term evolution (LTE) is considered one of the promising solutions to meet ever-increasing mobile traffic demand. Accordingly, 3GPP defines licensed-assisted access (LAA) in Release 13 to enable LTE operation in unlicensed band. Unlike conventional LTE utilizing licensed band exclusively, LAA has to overcome the fundamental barrier in unlicensed band—interference generated from other LAA devices or the incumbent systems like Wi-Fi. To address this coexistence issue, LAA has adopted listen-before-talk (LBT) channel access mechanism, resembling carrier-sense multiple access with collision avoidance (CSMA/CA) of Wi-Fi. The basic strategy of LBT is that, before starting a transmission, a transmitter "listens" the channel to ensure that the channel is idle, and hence, there is no on-going transmission. However, *contention collision* may occur if two or more transmitters see idle channel and transmit simultaneously. More importantly, it cannot be completely avoided, albeit LBT and CSMA/CA both reduce its occurrence by *exponential back-off*. Besides, *hidden collision* resulting from hidden terminals is another major cause of interference that cannot be mitigated by LBT.

By default, LTE adopts *adaptive modulation and coding* (AMC) to choose mod-

ulation and coding scheme index (MCS) used in downlink transmission, considering channel quality indicator (CQI) report provided by user equipment (UE). AMC operates well in licensed band because there is no unintended interference thanks to LTE's interference coordination technologies, i.e., inter-cell interference coordination (ICIC), enhanced ICIC (eICIC), and further eICIC (FeICIC). However, AMC does not fit LAA, which inevitably suffers from intermittent interference. Specifically, an LAA evolved Node B (eNB) will lower the MCS for the next transmission after encountering a collision, while the lowered MCS is preferable only if the next transmission suffers another collision. Put differently, if the eNB changes MCS based solely on the previous CQI report, it cannot fully exploit the transmission opportunities free from interference.

In this chapter, we propose collision-aware link adaptation (COALA), a zero-overhead and standard-compliant link-adaptation scheme, capable of efficiently exploiting the transmission opportunities, especially, when there is intermittent interference caused by contention and/or hidden collisions. COALA achieves its goal by gauging optimal MCS with *CQI discrimination*. eNB discriminates the CQI reports, whose values are dominated by temporal interference (due to collision), and hence, unable to reflect the actual channel quality. In essence, the CQI discrimination leverages the characteristics of the historical distribution of CQI reports, based on the observation that *the empirical distributions of CQI reports affected by interference and those free from interference show different shapes.* We adopt k-means clustering algorithm to differentiate them, and accordingly, by using the result of the CQI discrimination, COALA selects the optimal MCS considering whether the most recently received CQI is affected by collision interference as well as the estimated collision probability.

In summary, we claim the following contributions.

- We show that AMC, the default link-adaptation scheme of the conventional LTE, is not suitable for LAA in unlicensed band due to intermittent interference.
- We propose standard-compliant and zero-overhead link adaptation algorithm, COALA, which mitigates detrimental effect of intermittent interference on LAA's MCS se-

lection.

- We implement the CQI clustering and collision detection algorithm of COALA on our USRP-based LAA testbed, and show its effectiveness through prototype-based experiments.
- We extensively evaluate the performance of COALA through ns-3 simulations.

The rest of the chapter is organized as follows. We summarize background and related work in Section 3.2. The harmful impact of intermittent interference on AMC is discussed in Section 3.3. Then, we propose COALA in Section 3.4. In Section 3.5, we demonstrate the feasibility and effectiveness of COALA via prototype-based experiments and ns-3 simulation, respectively. We discuss several important points related to COALA in Section 3.6. Finally, we summarize the chapter in Section 3.7.

3.2 Backgound and Related Work

3.2.1 LAA and LBT

LAA is introduced by 3GPP to enable LTE operation in 5 GHz unlicensed band. It supports only downlink transmission using secondary component carrier (SCC) assisted by licensed primary component carrier (PCC) via carrier aggregation. Essentially, in the unlicensed band, multiple heterogeneous wireless technologies have to share the medium. In order to ensure a fair coexistence, LAA has adopted LBT operation, which resembles CSMA/CA of Wi-Fi. The LBT operation prescribes that LAA eNB should apply clear channel assessment (CCA) before starting transmission to avoid collision. Once an LAA eNB starts to transmit, it can occupy the channel for up to 8 ms, which is defined as maximum channel occupancy time (MCOT).

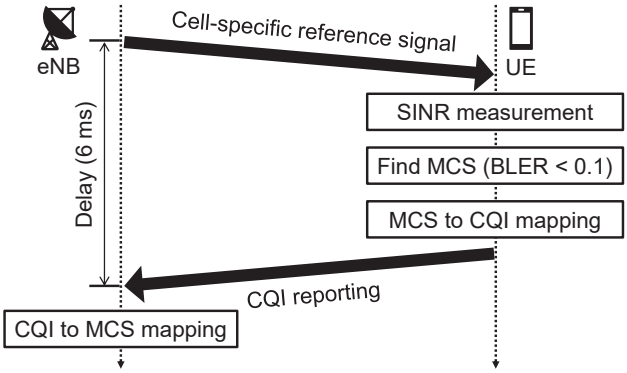

Figure 3.1: AMC illustration.

3.2.2 AMC

By default, LTE adopts AMC [34–37], which is illustrated in Fig. 3.1, where eNB adjusts MCS based on the CQI report provided by UE. In particular, eNB first transmits cell-specific reference signal (CRS) in every downlink subframe, and UE measures signal-to-interference-plus-noise ratio (SINR) based on the CRS. Afterwards, UE calculates the transport block error rate (BLER) based on the measured SINR in terms of each MCS. Finally, it selects the CQI associated with the highest MCS guaranteeing BLER under 10%, and reports the CQI to eNB via uplink channel.[1] Based on the CQI report, eNB adjusts MCS for the next downlink transmission. Besides, LTE supports both periodic and aperiodic CQI reporting. For FDD LTE, the periodic CQI reporting interval can be 2, 5, 10, 20, 32, 40, 64, 80, 128, and 160 ms, and the aperiodic CQI reporting can be triggered by CQI request from eNB.

3.2.3 Inter-Cell Interference Cancellation

To address inter-cell interference in licensed band, LTE has employed several versions of ICIC, i.e., ICIC, eICIC, and FeICIC. Thanks to these schemes, the negative impact

[1] 3GPP LTE standard defines MCS to CQI mapping [2, 36].

of inter-cell interference in licensed band can be eliminated or reduced significantly.[2] However, these schemes are effective only when interference is generated by eNBs from the same operator. That is, if interference is generated by eNBs from different operators or from different types of devices like Wi-Fi, the ICIC schemes cannot handle it, which is usually the case of LAA. The negative impact of interference on LAA in unlicensed band will be further discussed in Section 3.3.

3.2.4 Related Work

So far, there have been many efforts to improve LAA performance, where most of them focus on addressing the coexistence issues between LAA and Wi-Fi [7, 24, 38–41]. Besides, several studies have been reported to reflect the deficiency of the AMC when it is adopted by LAA. In [17], the authors point out that AMC is not feasible for LAA due to the inaccurate channel state information caused by the scarcity of the CRS in unlicensed band, and tackle the problem by periodically sending discovery reference signal (DRS), which embeds CRS. However, the impact of intermittent interference due to collision is not addressed in their work.

In [42], the authors indicate that the lowered MCS after encountering a collision can result in throughput reduction, and accordingly, propose a link-adaptation algorithm that adjusts MCS based on the signal-to-noise ratio (SNR) value only when there is no collision. They claim that collision can be detected by checking the difference between SNR and SINR based on the tacit assumption that SNR and SINR can be estimated using reference signal received power (RSRP) and reference signal received quality (RSRQ), respectively. However, we argue that SNR cannot be estimated using RSRP in unlicensed band. In licensed band, RSRP can reflect the SNR even if there is collision among CRSs, since neighboring cell's CRS can be eliminated with CRS interference cancellation (CRS-IC) of FeICIC. Therefore, a UE can measure RSRP

[2] Even if there is residual interference, its strength is weak and consistent such that AMC can work properly.

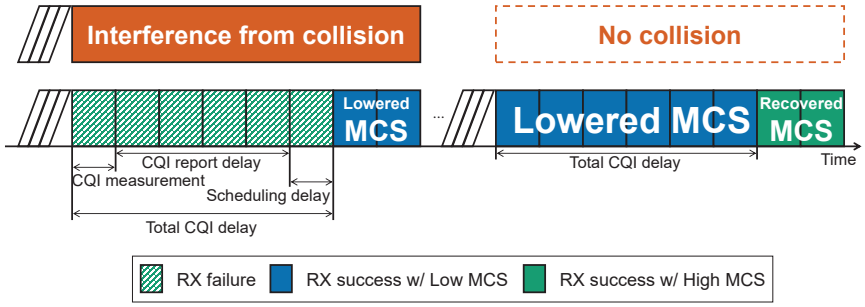

Figure 3.2: Unnecessary MCS lowering of AMC.

and infer the SNR in licensed band. However, for CRS-IC at the UE, eNB should provide a list of CRS-IC assistance information such as intra-frequency neighbouring cell's physical cell ID, the number of antenna ports, and multicast broadcast single frequency network (MBSFN) subframe configuration. In unlicensed spectrum, on the other hand, LAA eNB's CRS can collide with the CRS of eNBs from other operators and/or Wi-Fi signal, meaning that CRS-IC hardly works due to the absence of CRS-IC assistance information such that RSRP cannot be used to infer SNR.

3.3 Impact of Collision to Link Adaptation

Unlike licensed band, LAA suffers from contention collision or hidden collision interference in unlicensed band. Contention collision interference is inherently sporadic. Fig. 3.2 shows the AMC operation when a contention collision between two LAA signals occurs. If a UE measures CQI at the subframe which suffers from collision interference, the UE may report low CQI to the eNB due to low SINR measurement. However, when the eNB receives the CQI report from the UE, it is already 6 ms after contention collision interference has started. This is because of delays for CQI measurement, CQI report (UE processing), and eNB scheduling. Accordingly, even if the CQI is measured in the first subframe of the transmission (TX) burst whose maximum duration is 8 ms, only the last two subframes are transmitted using the lowered MCS.

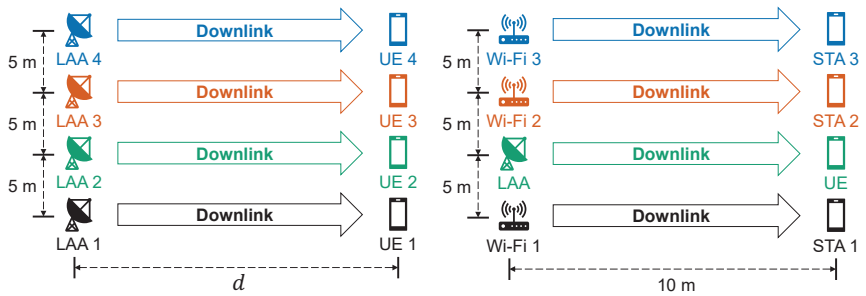

(a) Coexistence of LAA eNBs.

(b) Coexistence of an LAA eNB and Wi-Fi transmitters.

Figure 3.3: Simulation topology.

What makes this problem more complicated is the fact that the frontal subframes of the next TX burst will be transmitted by using this lowered MCS regardless of whether the next TX burst will experience collision interference or not. If the successive TX burst suffers from collision interference again, the UE may successfully receive this TX burst due to the lowered MCS. However, in general, the likelihood of the successive collision is not high. If the next TX burst experiences no collision interference, unnecessarily lowered MCS may harm spectral efficiency severely. Thus, lowering MCS can be a wrong choice when the collision probability is not significant. For example, if MCS has been dropped from 28 to 8 due to a CQI report from a collision-affected subframe, the spectral efficiency of next transmission will decrease from 5.5547 to 1.1758 [36]. The effective spectral efficiency, the spectral efficiency considering the success probability, of MCS 28 and MCS 8 will be about $5.5547 * (1 - P_{col})$ and 1.1758, where P_{col} is the collision probability. In this case, it is better to use MCS 28 unless P_{col} is greater than 0.79. Thus, AMC should handle these CQI reports which are affected by sporadic collision interference wisely to use the most suitable MCS in the unlicensed band.

Fig. 3.4 shows the operation of AMC for a different number of LAA eNBs, i.e.,

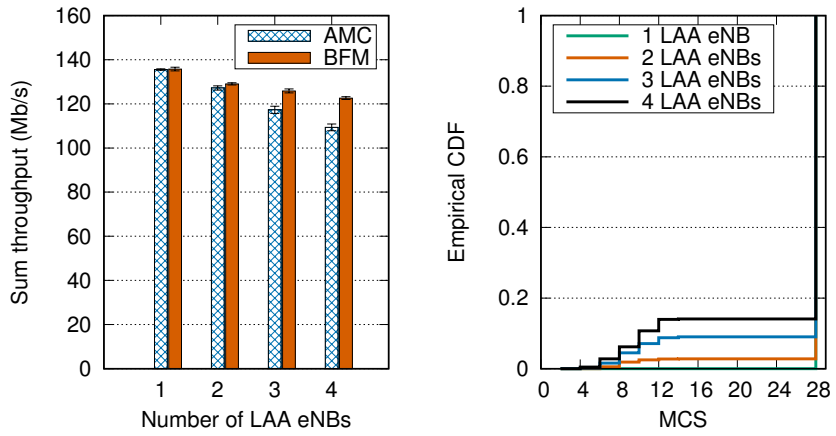

(a) Throughput degradation due to collision (b) Empirical CDF of MCS choices for different number of LAA eNBs.

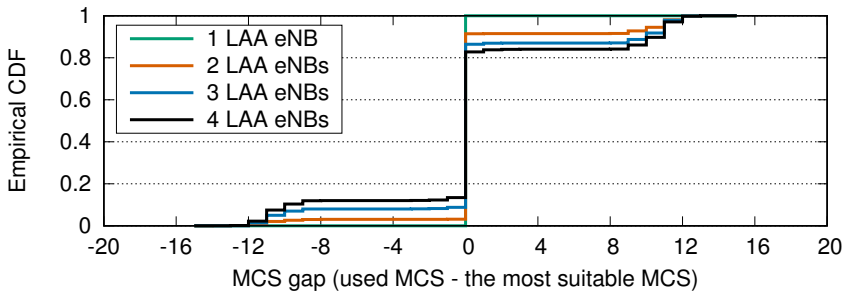

(c) Empirical CDF of MCS errors for different number of LAA eNBs.

Figure 3.4: The results in coexistence scenario of LAA eNBs.

a different level of contention collision probability.[3] LAA eNBs are 5 m apart from each other and the distance between the eNB and the UE is 10 m (see Fig. 3.3a). In this topology, all eNBs can detect transmission of each other. This means there are no hidden nodes. We use 2 ms periodic CQI reporting interval. See Section 3.5 for more detailed information of simulation setup. Fig. 3.4a shows the sum throughput performance when LAA eNBs adopt AMC for MCS selection and when LAA

[3]Contention collision probability is about 0.11, 0.19, and 0.24 for the numbers of coexisting LAA eNBs equal to 2, 3, and 4, respectively.

eNBs use the best fixed MCS (BFM) which have been found via brute-force search (in this case, MCS 28). The error bars show the standard deviations. The sum throughput gap between AMC and BFM increases as the number of coexisting LAA eNBs increases. AMC utilizes low MCS more frequently as the number of LAA eNBs increases as shown in Fig. 3.4b. The reason is that as more LAA eNBs coexist, more contention collisions occur and periodic CQI reports are more frequently affected by collision interference. Upon receiving the collision-affected CQI report, the eNB selects more robust MCS which can be successfully decoded even with collision interference. Fig. 3.4c illustrates distribution of *MCS gap*, defined as the used MCS minus the most suitable MCS which is found by a UE.[4] The negative value of MCS gap means that the eNB has used unnecessarily low MCS while the positive value means that the eNB has transmitted with high MCS but the channel is not good enough for the UE to successfully receive the eNB's transmission due to collision interference. As the number of coexisting LAA eNBs increases, the ratio of positive MCS gaps increases due to collision interference and the ratio of negative MCS gap values also increases due to unnecessarily low MCS usage.

Fig. 3.5 shows the normalized histogram of CQI reports from UEs. As illustrated in Fig. 3.5a, almost all CQI report values are 15 when one LAA eNB transmits alone. However, the portion of low CQI reports increases as the number of coexisting LAA eNBs increases. In Fig. 3.5a, we observe that there are two distinctive clusters where one cluster consists of CQI reports which are not affected by collision interference and the other is composed of CQI reports which are affected by the collision. In this chapter, the former cluster is called a *non-collision cluster*, and the latter cluster is called a *collision cluster*. Fig. 3.5b shows that the distribution of non-collision cluster changes as the distance between eNBs and UEs (d) changes, but still can be distinguished from collision cluster. Of course, non-collision cluster can be overlapped with

[4]The most suitable MCS is the highest MCS whose estimated BLER remains under 10% based on the received SINR at the subframe.

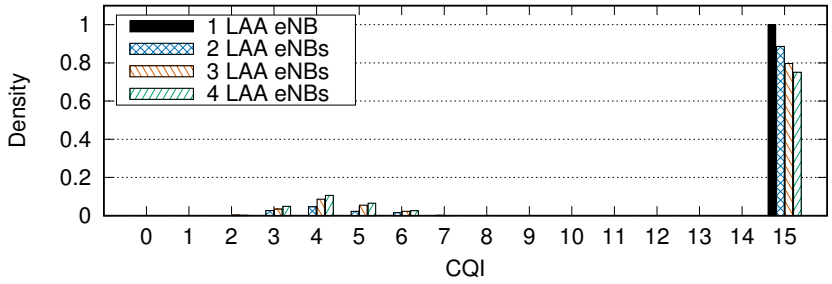

(a) Normalized histogram of CQI reports for different number of LAA eNBs ($d = 10$).

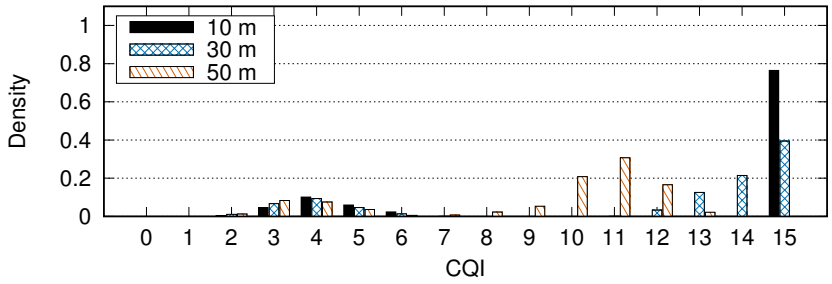

(b) Normalized histogram of CQI reports for different distance d between eNB and UE.

Figure 3.5: Normalized histogram of CQI reports.

collision cluster under certain circumstances, but it can also be interpreted that the impact of collision interference is not significant in such an environment.

Fig. 3.6 shows the performance of AMC with three contending 802.11ac Wi-Fi transmitters. Fig. 3.6a illustrates the throughput performance of the LAA eNB which exploits AMC, for different time interval of periodic CQI report. With 2 ms time interval of periodic CQI report, the throughput performance of AMC does not decrease when Wi-Fi transmitters coexist with an LAA eNB, unlike when there are only LAA eNBs. This is because 802.11ac Wi-Fi interference is likely shorter than MCOT duration of LAA (i.e., 8 ms)[5] and accordingly the latter subframes in MCOT duration

[5]Maximum physical protocol data unit (PPDU) duration of 802.11ac Wi-Fi is 5.484 ms. Many commercial off-the-shelf 802.11n devices use 4 ms for its default maximum PPDU duration, while 802.11n specification defines maximum PPDU duration as 10 ms.

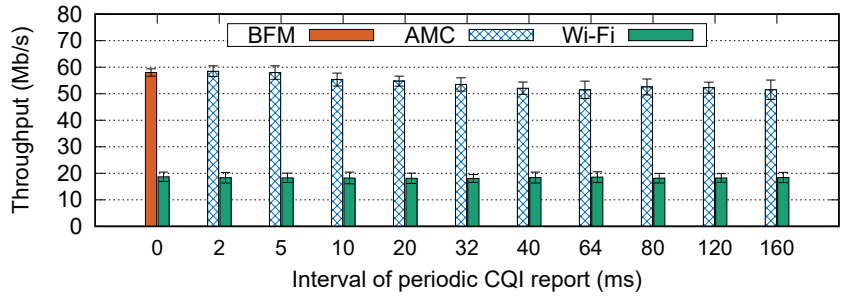

(a) Throughput degradation for different time interval of periodic CQI report.

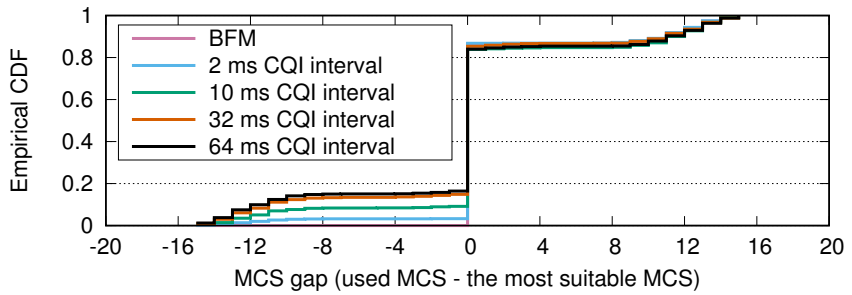

(b) Empirical CDF of MCS errors for different time interval of periodic CQI report.

Figure 3.6: The results in coexistence scenario of 1 LAA eNB and 3 Wi-Fi transmitters.

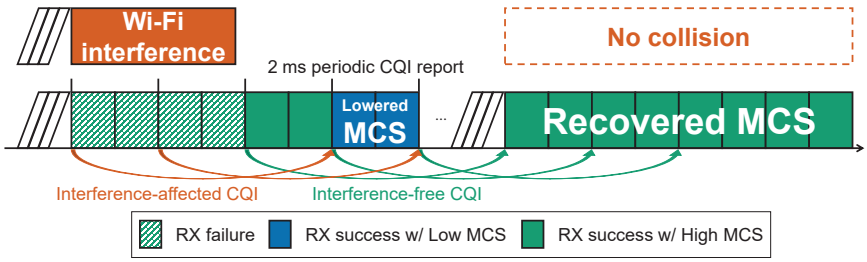

Figure 3.7: Collision with relatively short Wi-Fi frame.

may not suffer from contention collision interference. If the time interval of periodic CQI report is 2 ms, the last CQI measurement and report in the MCOT duration is performed at the subframe which is not affected by contention collision. Fig. 3.7 shows the CQI reporting and MCS selection when a transmission of LAA collides with a relatively short Wi-Fi frame. However, if the time interval of periodic CQI report is

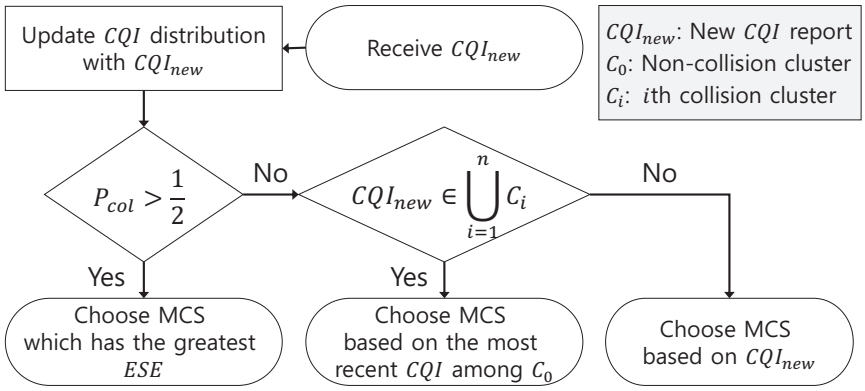

Figure 3.8: Flow chart of COALA.

longer than 2 ms (i.e., $5, 10, \cdots, 160$ ms), there is a possibility that the CQI measurement is not performed at the latter subframes in MCOT duration which do not suffer from collision interference. Fig. 3.6a shows that the throughput of AMC is lower than BFM when the time interval of periodic CQI report is greater than 2 ms. In Fig. 3.6b, we observe that there are more negative MCS gap values as the time interval of periodic CQI report increases, which means that AMC selects unnecessarily low MCS more as the time interval of periodic CQI report increases.

3.4 COALA: Collision-aware Link Adaptation

In this section, we propose a novel link adaptation algorithm, COALA, which mitigates harmful effect of intermittent interference on MCS selection due to collisions in unlicensed band without any additional protocol overhead. As we have discussed in Section 3.3, AMC cannot operate properly in the collision-prone environment. To address the problem, COALA estimates the future collision probability and checks whether the most recent CQI report is affected by collision interference or not. Based on those information, COALA selects MCS which will be used for next data transmission.

3.4.1 CQI Clustering Algorithm

COALA utilizes the distribution of past CQI reports to determine if the received CQI is affected by collision. If the strength of collision interference is not negligible, CQI reports suffering from the collision exhibits a different distribution from the non-collided CQI reports as shown in Fig. 3.5.

COALA leverages k-means clustering algorithm which is one of the simplest unsupervised learning algorithms [43]. k-means clustering algorithm divides data into k clusters by solving (3.1).

$$\underset{\mathbb{C}}{\operatorname{argmin}} \sum_{i=1}^{k} \sum_{x \in C_i} \|x - \mu_i\|^2, \tag{3.1}$$

where x, μ_i, C_i, k, and $\mathbb{C}$ are the data value (the CQI report value, in our application), the centroid of the ith cluster, the ith cluster, the total number of clusters, and the set of all clusters, respectively. The major problem with k-means clustering is to determine the number of clusters (k) in a data set. In general, choosing k correctly is a difficult problem, because increasing k will always reduce the amount of error in the clustering result. To tackle the problem, we leverages the *gap statistic* method [44], which compares the dispersion level of clustered data with that of clustered null reference distribution. The estimated optimal number of clusters is a value that maximizes the difference between the dispersion levels. Then, CQI reports are divided into clusters, where the cluster number is determined by the *gap statistic* method.

3.4.2 Collision Detection and Collision Probability Estimation

COALA can estimate future collision probability based on clustering results of past CQI reports. If there is only one cluster, LAA eNB can notice that future transmission is not likely to collide with the transmission of others. On the other hand, if there are two or more clusters, LAA eNB can infer that there is a possibility of collisions in future transmission. In this chapter, this is called *collision detection*.

Furthermore, the LAA eNB can calculate estimated collision probability by comparing the size of the cluster of CQI reports which are not affected by collision (non-collision cluster, C_0) and the sum size of the other clusters (collision clusters, $C_i, 1 \leq i \leq n$, where n is the number of collision clusters). Non-collision cluster is a cluster which has the highest mean CQI value. The size of the ith cluster (S_i) can be calculated as follows:

$$S_i = |C_i| = \sum_{j=\min(C_i)}^{\max(C_i)} N_j, \tag{3.2}$$

where N_j, C_i, $\min(C_i)$, and $\max(C_i)$ are the number of CQI reports whose value is j, the ith cluster, the minimum CQI value of C_i, and the maximum CQI value of C_i, respectively. Estimated collision probability can be calculated as follows:

$$P_{col} = 1 - \frac{S_0}{\sum_{i=0}^{n} S_i}, \tag{3.3}$$

where S_0 and S_i are the size of the non-collision cluster and the size of the ith collision cluster, respectively.

3.4.3 Suitable MCS Selection

If P_{col} is less than or equal to 1/2, future transmission of the eNB is more likely to be successfully without collision interference. In this case, upon reception of a new CQI report, COALA checks which cluster the received CQI report belongs to. If the received CQI report is found to be in one of the collision clusters, COALA chooses MCS based on the latest CQI report which is in the non-collision cluster instead of the received CQI report. By utilizing the CQI report from the non-collision cluster, the eNB can avoid spectral efficiency degradation due to unnecessarily low MCS selection when no collision occurs in the next transmission. If the received CQI report is in non-collision cluster, COALA uses the CQI report for the next transmission just like AMC does.

On the other hand, if P_{col} is greater than 1/2, COALA takes a different strategy for MCS selection. COALA calculates effective spectral efficiency for every MCS which

can be selected based on CQI report. Effective spectral efficiency (ESE_q) of MCS which corresponds to CQI q can be calculated as follows:

$$ESE_q = SE_q \times \frac{\sum_{j=q}^{15} N_j}{\sum_{j=0}^{15} N_j}, \tag{3.4}$$

where SE_i is spectral efficiency of MCS which corresponds to CQI i. We estimate the success probability of MCS which corresponds to CQI q as the number of past CQI reports whose values are greater than or equal to q over the number of all past CQI reports. COALA leverages CQI value which has the highest effective spectral efficiency for MCS selection. Fig. 3.8 outlines the operation flow of COALA.

3.5 Performance Evaluation

We implement the CQI clustering and collision detection algorithm of COALA in our LAA testbed for the feasibility study. We use the NI USRP-2943R device which has Xilinx Kintex-7 FPGA and the host desktop computer which has the Intel i7 3.3 GHz processor. Buffalo WZR-HP-AG300H 802.11n AP, which has the Qualcomm Atheros AR9220 chipset, is used for the coexisting Wi-Fi transmitter node.

We also evaluate the performance of COALA via ns-3 simulation. We have implemented an coexistence model between LAA and Wi-Fi in *ns-3.22* [27], where LTE and Wi-Fi models are implemented separately in the original version. In particular, following features have been implemented: Interference between LAA and Wi-Fi, multiple-input multiple-output (MIMO) for LAA and Wi-Fi, LBT, reservation signal, initial and ending partial subframe, 3GPP indoor hotspot channel model, and 3GPP file transfer protocol (FTP) traffic model [3]. In 3GPP FTP model, 0.5 MB files arrive according to a Poisson process. User datagram protocol (UDP) is used for file transmission. We make all transmitters have saturated traffic and set the CQI observation window size to 200 unless stated otherwise. The detailed simulation settings are summarized in Table 3.1.

Table 3.1: Simulation settings for Chapter 3 evaluation.

Simulation settings	Value
Simulation time	10 s
Number of iterations	10
File size	0.5 MB
Bandwidth	20 MHz
Wi-Fi PHY	802.11ac, 2×2 MIMO
Wi-Fi guard interval	800 ns
Wi-Fi maximum A-MPDU bound	5.484 ms, 1,048,575 B
Wi-Fi rate adaptation	Minstrel VHT
AP/eNB transmission power	23 dBm
STA/UE transmission power	23 dBm
Wi-Fi CS/CCA threshold	−82 dBm
Wi-Fi CCA-ED threshold	−62 dBm
LAA CCA-ED threshold	−72 dBm

3.5.1 Prototype-based Feasibility Study

We first check whether the unsupervised clustering and collision detection of COALA work well in the real environment. We deploy the NI USRP which has the LAA system (i.e., a pair of LAA eNB and LAA UE) and three commercial off-the-shelf Wi-Fi APs in an office environment (see Fig. 3.9). In this measurement study, the LAA UE feeds back CQI reports with 10 ms periodicity. Each Wi-Fi AP transmits downlink traffic to a nearby Wi-Fi station (STA). We have conducted our experiments with a 20 MHz operating channel (channel number 44 with 5.22 GHz center frequency) and all measurements have been performed for 10 min.

Fig. 3.11 shows the distribution of CQI reports from the LAA UE. When the LAA system coexists with three Wi-Fi APs, the size of the collision cluster (the number of

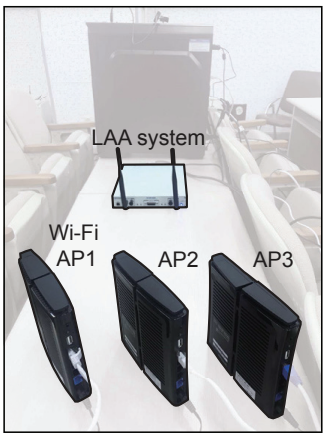

Figure 3.9: Testbed.

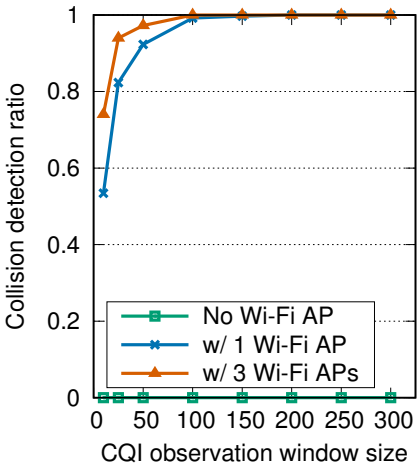

Figure 3.10: Collision detection performance of COALA.

CQI reports whose value is 11 or less) increases compared to when the LAA system coexists with one Wi-Fi AP. This means that more collisions have occurred when the LAA eNB competes with three Wi-Fi APs.

Fig. 3.10 illustrates the collision detection performance of COALA. The *CQI observation window size* is the number CQI reports which are used for COALA's collision detection and MCS selection. If the CQI observation window size is insufficient, collision-affected CQI reports can be quickly forgotten. If there is no contending Wi-Fi AP, COALA detects no collision regardless of CQI observation window size. In this case, COALA selects MCS in the same way as AMC. On the other hand, the collision detection ratio decreases as the CQI observation window size decreases. If the CQI observation window size is small, the collision detection ratio of COALA when coexisting with one Wi-Fi AP is lower than that when coexisting with three Wi-Fi APs. This is because, when the LAA eNB coexists with a single Wi-Fi AP, the collision probability is much lower and the probability of collisions being observed in the CQI window is also low. However, the collision detection ratio of COALA is close to one with the CQI window size of 150 or more, regardless of the number of coexisting WI-Fi APs.

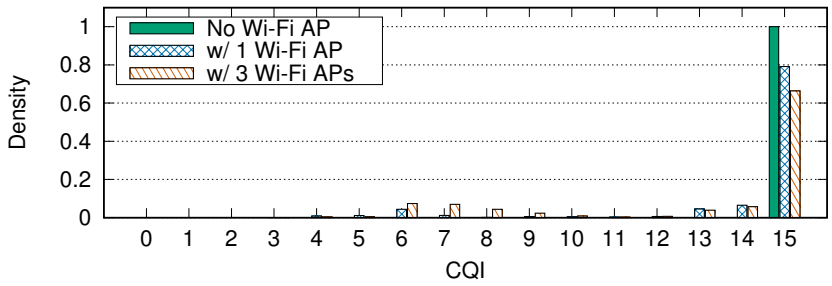

Figure 3.11: Normalized histogram of CQI reports.

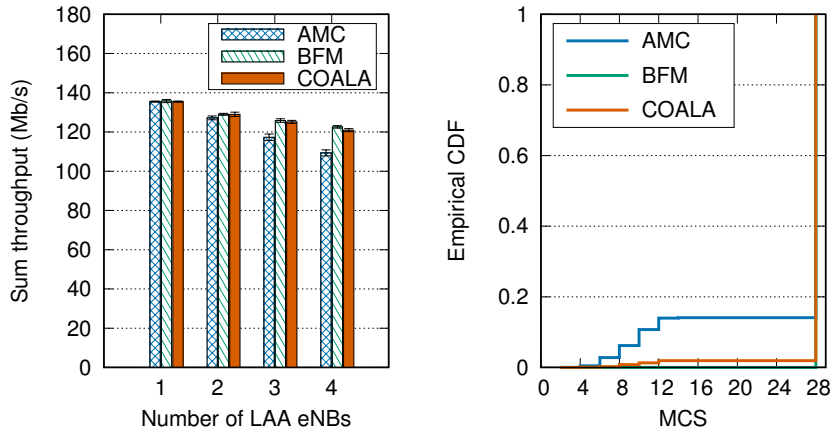

(a) Throughput performance for different number of LAA eNBs.

(b) Empirical CDF of MCS selection when four LAA eNBs coexist.

Figure 3.12: Performance of COALA.

3.5.2 Contention Collision with LAA eNBs

We evaluate COALA in a scenario where multiple LAA eNBs coexist. We deploy up to four pairs of a single eNB and a UE as illustrated in Fig. 3.3a. Each eNB-UE pairs are 5 m apart from each other (no hidden terminals in this topology).

Fig. 3.12a shows the sum throughput performance of COALA as the number of coexisting eNBs increases. As the number of eNBs increases, more collisions occur and the sum throughput of LAA eNBs decreases. Collision not only prevents suc-

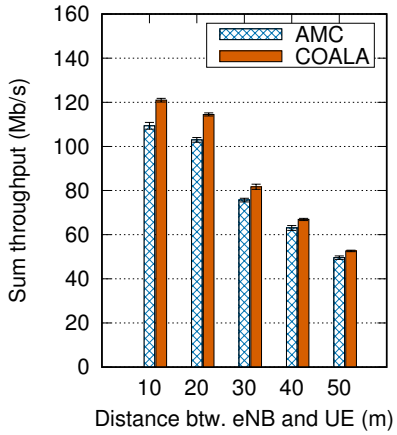

Figure 3.13: Throughput performance of AMC and COALA for different distance between eNB and UE.

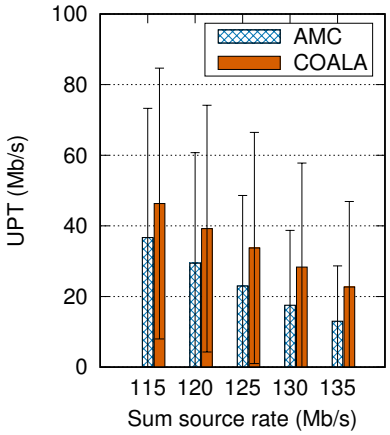

Figure 3.14: UPT performance of AMC and COALA for unsaturated traffic with different source rate.

cessful data reception, but also prevents AMC from choosing the most suitable MCS. Sum throughput performance is reduced more steeply when LAA eNBs utilize AMC for MCS selection than BFM. This sum throughput degradation of AMC implies that AMC cannot select appropriate MCS when collision can occur. On the other hand, sum throughput of LAA eNBs which leverage COALA is very close to that of LAA eNBs which use BFM. The sum throughput gain of COALA over AMC is 10.6% when four LAA eNBs coexist. In Fig. 3.12b, we observe that COALA hardly chooses low MCS, whereas AMC uses low MCSs for about 14% of transmission.

Fig. 3.13 illustrates that the sum throughput performance of COALA is greater than that of AMC regardless of the distance between eNBs and UEs. In this scenario, the path-loss values are 69.09, 82.12, 89.75, 95.16, and 99.35 dB for 10, 20, 30, 40, and 50 m, respectively. Sum throughput gain of COALA increases as the distance between eNBs and UEs decreases. This is because the greater the difference in CQI report between when there is a collision and when there is no collision, the greater the throughput loss caused by the inappropriate MCS selection of AMC.

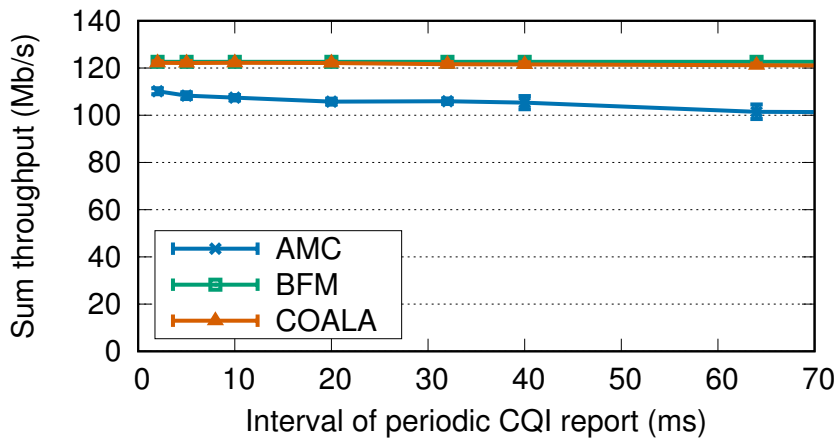

Figure 3.15: Throughput performance of COALA for different time interval of periodic CQI report.

Fig. 3.14 compares the user perceived throughput (UPT) performance of COALA with AMC, when each LAA eNBs have unsaturated traffic. UPT is the average of all file throughput values which can be calculated by dividing the received file size by the time between the arrival of the first packet of the file and the reception of the last packet of the file [3]. The UPT gain of COALA over AMC is 26.2, 33.0, 46.7, 61.5, and 74.7% when four LAA eNBs' sum source rate is 115, 120, 125, 130, and 135, respectively.

Fig. 3.15 shows the impact of the time interval of periodic CQI report on the operation of COALA when four LAA eNBs coexist. The throughput degradation of AMC increases as the time interval of periodic CQI reporting increases. This is because the effect of the CQI report lasts longer as the time interval increases. In Fig. 3.15, we observe that COALA operates well regardless of the CQI reporting time interval and the sum throughput gain of COALA over AMC increases as the time interval of periodic CQI report increases.

An insufficient CQI observation window size can degrade collision detection performance. On the other hand, with the oversized CQI observation window, it may

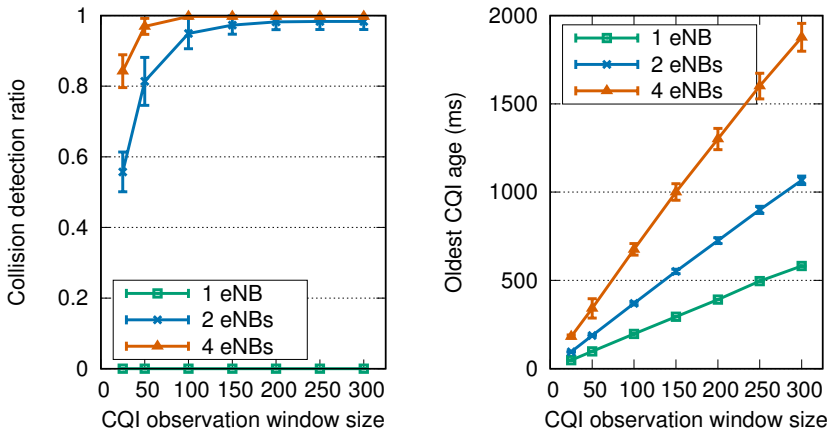

(a) Collision detection ratio.

(b) Age of the oldest CQI report.

Figure 3.16: Impact of the CQI observation windows size on collision detection of COALA.

be difficult for COALA to react quickly to environmental changes (e.g., change of path loss and/or disappearance of collisions). Fig. 3.16a shows the impact of the CQI observation window size to COALA's collision detection performance. We see that COALA's collision detection ratio decreases as the CQI observation window size decreases. When two LAA eNBs coexists, the probability of collisions being observed in the CQI window is low and the collision detection ratio becomes also low. Collision detection ratio is very close to one when the CQI observation window size is greater than or equal to 200.

COALA keeps CQI reports longer as the CQI observation window size increases. Fig. 3.16b illustrates that the oldest CQI age, i.e., the elapsed time since the oldest report in the CQI observation window has been received, increases as the CQI observation window size increases. However, it is shown that the oldest CQI age does not exceed 2 s, thus preventing too outdated CQI report being used.

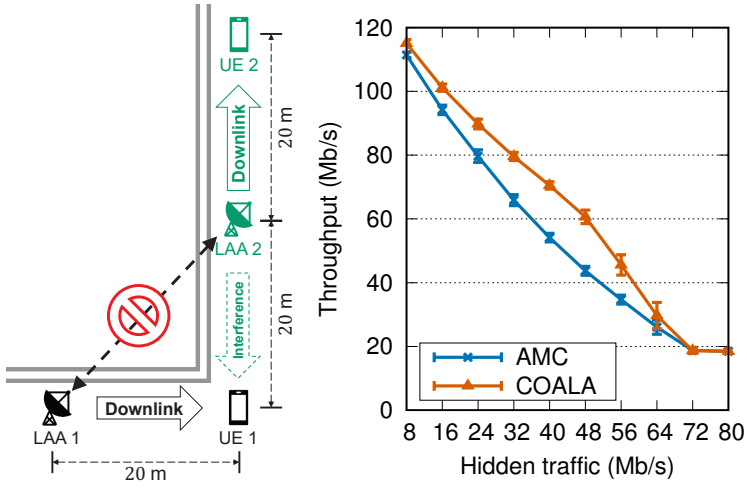

(a) Topology.

(b) Throughput performance of COALA for different source rate of LAA eNB 2.

Figure 3.17: Hidden collision scenario.

3.5.3 Hidden Collision

We evaluate the throughput performance of COALA in hidden collision scenario. As shown in Fig. 3.17a, LAA eNBs 1 and 2 cannot sense transmission of each other, while UE 1 may suffer from the interference of LAA eNB 2. Fig. 3.17b shows the throughput performance of LAA eNB 1 with various source rate of LAA eNB 2 while LAA eNB 1 is fully loaded. To generate various source rates (8–80 Mb/s), we reduce file size to 50 KB and vary file arrival rate (40–200 files/s). We can observe that COALA and AMC show similar throughput performance when the source rate of LAA eNB 2 is over 72 Mb/s. The reason is that if the hidden traffic source rate is very high, most subframes may suffer from hidden collisions and there is little chance of an incorrect MCS selection in AMC. However, COALA achieves higher throughput than AMC when the source rate of hidden traffic is lower than 72 Mb/s. Especially with 48 Mb/s hidden traffic, the throughput gain of COALA over AMC is 38.6%.

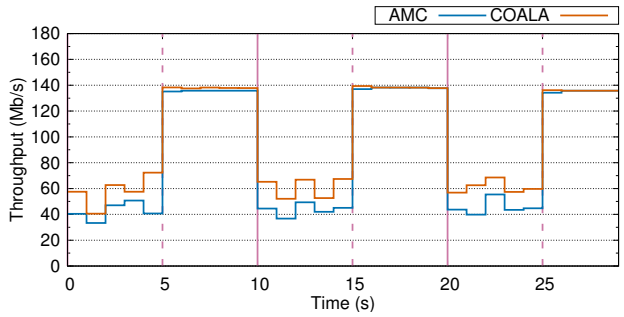

(a) Throughput performance.

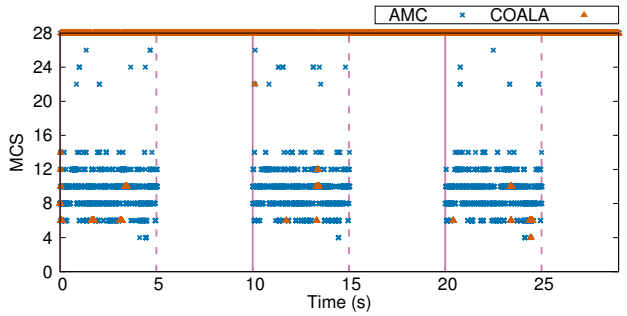

(b) Trace of MCS usage.

Figure 3.18: Bursty hidden collision scenario.

3.5.4 Bursty Hidden Collision

Fig. 3.18 illustrates behavior of COALA in case of bursty hidden collision scenario. Solid and dotted vertical lines represent the start and the end of hidden traffic, respectively. In Fig. 3.18a, the LAA's throughput deteriorates with the hidden traffic, but COALA can alleviate the throughput degradation. This is because COALA rarely uses low MCSs which are robust but achieve poor spectral efficiency (see Fig. 3.18b).

3.5.5 Contention Collision with Wi-Fi Transmitters

Fig. 3.19 shows the throughput performance of COALA when an LAA eNB coexists with three Wi-Fi transmitters. As we have discussed in Section 3.3, the longer the time interval of periodic CQI reporting, the greater the LAA throughput degradation

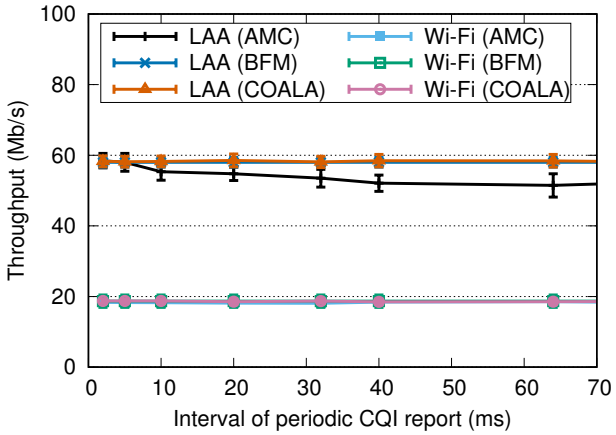

Figure 3.19: Throughput performance of COALA for different time interval of periodic CQI report.

of AMC. Meanwhile, the LAA throughput of COALA does not decreases as the time interval of periodic CQI reporting increases and shows almost the same LAA throughput with BFM. The Wi-Fi throughput does not change regardless of time interval of periodic CQI reporting or an LAA link adaptation algorithm.

3.6 Discussion

Standard compliance & zero overhead: COALA is fully compliant to the state-of-art 3GPP LAA standard. COALA only uses the CQI reports which are already reported by conventional LTE or LAA UEs. Thus, COALA does not incur any overhead for detecting collisions and selecting the most suitable MCS.

Computational complexity: k-means clustering algorithm is one of the simplest unsupervised learning algorithms. The computational complexity of k-means clustering algorithm is known as $O(nkdi)$, where n is the number of vectors, k is the number of clusters, d is the number of dimension of vectors, and i is the number of iterations required to converge [45, 46]. Because we deal with 1-dimensional CQI report data whose maximum number is the size of observation window, the computational

complexity of k-means clustering in COALA is $O(nki)$. Because we use *gap statistic* method to find the optimal number of clusters, we have to run k-means clustering algorithm for $k = 1, 2, \cdots, m$, where m is the maximum number of clusters. As a result, the computational complexity of COALA is $O(ni \times \frac{m(m+1)}{2})$. However, in COALA, i and m are relatively small to n. (In this chapter, we use 5, 3, and 200 as i, m, and n values, respectively.) Thus, we can say that $O(ni \times \frac{m(m+1)}{2}) = O(n)$.

Multiple non-collision clusters: We assume that there is only one non-collision cluster. If the path loss between the LAA eNB and the LAA UE changes significantly within COALA's observation window, there can be multiple non-collision clusters. However, it should be rare event in practice, because COALA forgets past CQI reports which have been received a few seconds ago. Consider the pedestrian's walking speed (about 1.3 m/s), significant path loss change rarely occurs in a few seconds. Even if the path loss has changed in such a short time, COALA will forget stale CQI reports of the previous collision cluster in a few seconds.

Different MCOT values: We assume that MCOT is 8 ms which are used for channel access priority classes 3 and 4 [2]. However, the MCOT value is 2 ms and 3 ms for priority classes 1 and 2, respectively, and the MCOT value cannot exceed 4 ms in Japan. When LAA's MCOT is shorter than Wi-Fi's maximum PPDU duration (e.g., 5.484 ms for 802.11ac frame), the entire subframes in MCOT are more likely to be interfered by collision with a Wi-Fi frame. This can increase the likelihood that AMC chooses a wrong MCS even if the time interval of periodic CQI report is very short (i.e., 2 ms) and the gain of COALA over AMC with the short time interval of periodic CQI report is expected to increase.

3.7 Summary

In this chapter, we have proposed COALA to mitigate the impact of collisions to MCS selection. We first show that AMC, the conventional link adaptation of LAA, does

not operate well in unlicensed band due to collisions. To solve this problem, COALA detects collision based on unsupervised clustering and takes different MCS selection strategies depending on whether a received CQI report is affected by a collision or not. By doing so, COALA can avoid the usage of unnecessarily low MCS. Our implementation and simulation verify the feasibility and the performance of COALA in various scenarios. COALA improves the LAA throughput by up to 10.6% and the LAA UPT by up to 74.7% when four LAA eNBs coexist. COALA also yields the LAA throughput improvement of up to 38.6% when there are hidden collisions. As future work, we plan to extend our algorithm for uplink transmission of LAA.

Chapter 4

PETAL: Power and Energy Detection Threshold Adaptation for LAA

4.1 Introduction

In unlicensed spectrum, all transmitters should detect the channel before using the spectrum and transmit only if the spectrum is detected as idle. To detect signals of co-existing devices which utilizes different wireless technologies, devices compare measured energy level of the signals to a specific threshold, so-called energy detection threshold. However, the energy detection procedure operates on the transmitter side and does not consider signal quality at the receiver side. This brings a exposed node problem which is a notorious problem in the unlicensed spectrum. Exposed node problem occurs when transmitters cannot transmit during another transmitter's transmission, due to the detected energy level of the other transmitter exceeds energy detection threshold, but their receivers are relatively far from the other transmitter so skipping transmission results in spectral efficiency loss.

3GPP standard specifies the maximum value of LAA's energy detection threshold which depends on the eNB transmission power and bandwidth usage. So, we design a baseline algorithm which can adjust its energy detection threshold at the observed

power of the ongoing transmission and transmit its own signal with reduced power if the eNB observes another device's transmission during backoff procedure. We call this operation as spatial reuse (SR) in this chapter. The rationale behind this is that the eNB can access the channel more aggressively as it is less likely to interfere with other devices. However, reducing transmission power and transmitting signal simultaneously with the other device's transmission may not be a good decision if the receiver is close to an interferer and received SINR will drop dramatically.

In this chapter, we propose a power and energy detection threshold adaptation (PETAL) algorithm, a zero-overhead and standard-compliant power and energy detection threshold adaptation scheme, which utilizes CQI reports from UE. PETAL predicts and compares the spectral efficiency when the eNB performs SR and when it does not. PETAL performs SR only if the spectral efficiency of SR is expected to be higher than in the case of non-SR.

In summary, the main contribution of the chapter is as follows.

- We design a baseline algorithm, which operates similar to overlapping basic service set packet detection (OBSS-PD) operation of IEEE 802.11ax, and show that the baseline algorithm causes the throughput degradation when the UE is close to an interferer.
- We propose a power and energy detection threshold adaptation algorithm, PETAL, which performs SR wisely and mitigates the deleterious effect of SR while the UE is likely to suffer from severe interference.
- We extensively evaluate the performance of PETAL through ns-3 simulations.

The rest of the chapter is organized as follows. We summarize background and related work in Section 4.2. In Section 4.3, we design a baseline algorithm which operates spatial reuse aggressively and show that the baseline algorithm degrades the throughput performance severely when the UE is close to an interferer. Then, we propose PETAL in Section 4.4. In Section 4.5, PETAL is evaluated via ns-3 simulation.

Finally, we summarize the chapter in Section 4.6.

4.2 Backgound and Related Work

4.2.1 Energy Detection Threshold

For spectrum sensing, Wi-Fi and LAA leverage energy detection technique to detect signals between different wireless technology. The energy detection technique measures the energy level of the channel and compares the value with the specific energy detection threshold. Then, the energy detection technique determines that the channel is busy only if the measured energy level exceeds the energy detection threshold. LAA can adapt the energy detection threshold according to the transmission power, while Wi-Fi has a fixed value of energy detection threshold, i.e., -72 dBm. 3GPP standard defines that the energy detection threshold for 20 MHz carrier bandwidth should be less than or equal to the maximum energy detection threshold ($X_{\mathrm{Thres\_max}}$) which is determined as below:

$$X_{\mathrm{Thres\_max}} = \max \begin{cases} -72 \text{ dBm}; \\ \min \begin{cases} -62 \text{ dBm}; \\ -72 + (23 - P_{TX}) \text{ dBm}, \end{cases} \end{cases} \tag{4.1}$$

where P_{TX} is the transmission power.

4.2.2 Related Work

The impact of a different energy detection threshold of LAA is studied in [15, 47, 48]. In [15], Jeon *et al.* observed that proper controlling the energy detection threshold and a contention window size of LAA can balance the performance between Wi-Fi and LAA systems. The authors in [47] analyzed the coexistence performance of Wi-Fi and LAA via stochastic geometry and found that proper selection of energy detection thresholds is beneficial to coexistence. In [48], Falconetti *et al.* discussed the impact

of parameters of LAA including an energy detection threshold and mentioned that a higher energy detection threshold can enable more spatial reuse but introduce higher interference. The authors also mentioned that there is the optimal energy detection threshold dependent on the deployment specifics.

In [49], Li *et al.* proposed an enhanced LBT scheme which adaptively adjusts the energy detection threshold to guarantee the fair coexistence with Wi-Fi while providing enhanced performance for LAA. The proposed algorithm increases the energy detection threshold step by step if the detected power of the signal from an intra-operator eNB is above -70 dBm. The proposed scheme does not adjust the energy detection threshold if the detected Wi-Fi signal power is above -70 dBm to protect the Wi-Fi networks which are more vulnerable to interference. However, the proposed algorithm is not compliant with 3GPP standard because the algorithm does not adjust the transmission power to the corresponding energy detection threshold. Furthermore, the algorithm assumes that the eNB knows the interference power from adjacent transmitters, which is very impractical.

In [11], Sagari *et al.* made an optimization framework which exploits power control for the aggregate throughput maximization when Wi-Fi and LTE-U networks coexist. However, unlike our proposed algorithm, their proposed framework adjusts the transmission power levels of Wi-Fi and LTE-U networks once and then it does not change the transmission power level. Furthermore, the authors assume network state information exchange between every coexisting networks which is very unlikely in the real environment.

4.3 Baseline Algorithm

4.3.1 Design of the Baseline Algorithm

We design a baseline algorithm which is similar to the OBSS-PD operation of IEEE 802.11ax. When the signal of neighboring devices are observed with the energy level

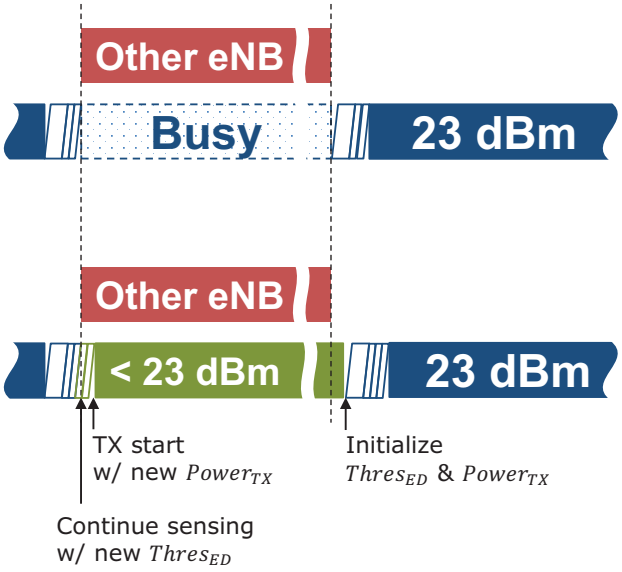

Figure 4.1: Baseline algorithm illustration.

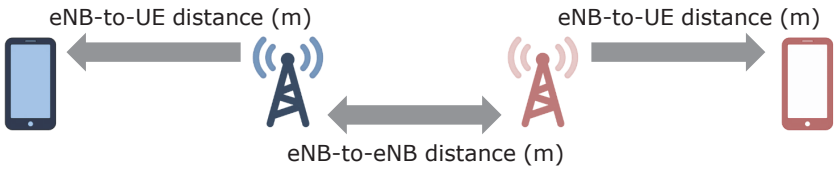

Figure 4.2: Simulation topology for two cell scenario.

between -72 dBm and -62 dBm, the baseline algorithm adjusts its energy detection threshold to the observed energy level and continues backoff procedure while standard LAA determines that the channel is busy. When the backoff counter reaches zero with a modified energy detection threshold, the baseline algorithm starts transmission with reduced transmission power. The proposed algorithm resets the energy detection threshold and transmission power after every transmission.

4.3.2 Performance of the Baseline Algorithm

Figs. 4.3 and 4.4 show the throughput performance of standard LAA and the baseline algorithm, respectively. Simulation topology is illustrated in Fig. 4.2. There are two

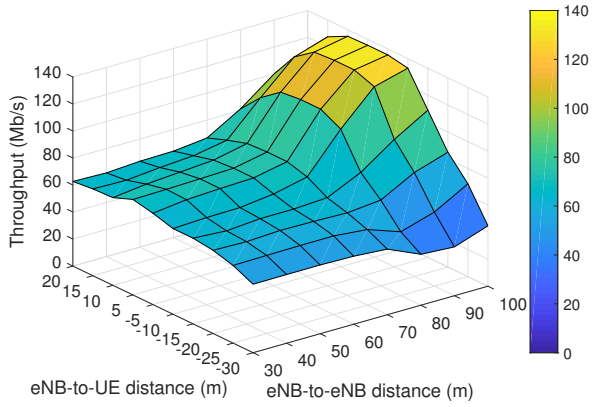

Figure 4.3: Throughput performance of standard LAA.

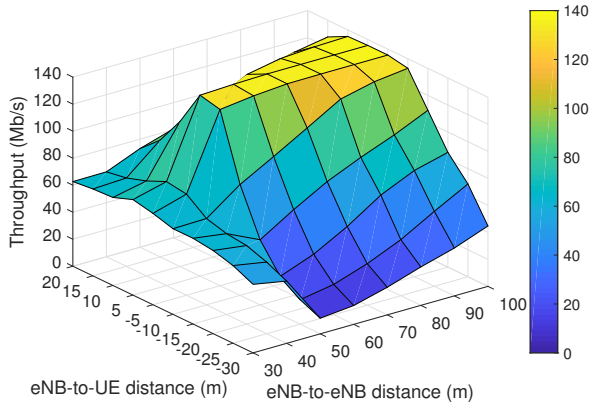

Figure 4.4: Throughput performance of baseline algorithm.

eNB/UE pairs of different operators. The minus value of eNB-to-UE distance means that the UE is between eNBs. At first glance, we can see the throughput enhancement of the baseline algorithm where the eNB-to-UE distance is short and the eNB-to-eNB distance is not very short or very long. In this topology, when the eNB-to-eNB distance is between 40 m and 60 m, each other eNB's signal can be observed with an energy level between -72 dBm and -62 dBm and accordingly the baseline algorithm operates SR. However, when the eNB-to-UE distance is far from its own eNB and near to the other eNB, the throughput performance degrades severely. This is because of the fact

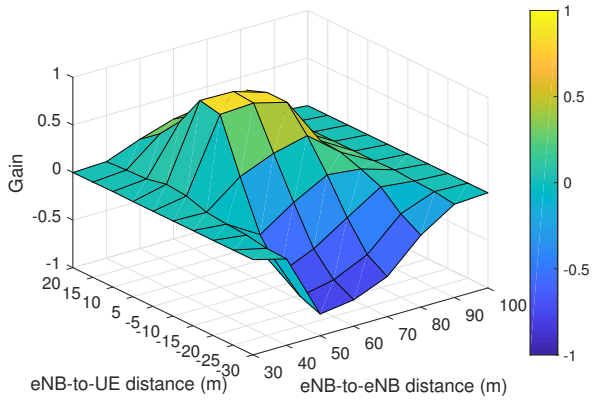

Figure 4.5: Gain of baseline algorithm over standard LAA.

that the transmission of the other operator's eNB interferes critically and SINR of the signal from its own eNB decreases. In this case, it is better not to do SR because the loss from lowered SINR is much greater than the gain from additional airtime usage. Fig. 4.5 shows the gain of baseline over standard LAA. The gain is about 0.86 and -0.77 when the eNB-to-eNB distance is 50 m and the eNB-to-UE distance is 5 m and when the eNB-to-eNB distance is 50 m and the eNB-to-UE distance is -30 m, respectively.

4.4 PETAL: Power and Energy Detection Threshold Adaptation

In this section, we propose a power and energy detection threshold adaptation algorithm, PETAL, which performs SR wisely and mitigates the negative effect of SR while the UE is likely to suffer from severe interference without any additional protocol overhead. As we have discussed in Section. 4.3, the baseline algorithm which operates SR whenever the energy level of the observed signal is between -72 dBm and -62 dBm may improve or worsen the throughput performance depending on the situation. More specifically, if the loss from lowered SINR is much greater than the gain from ad-

ditional airtime usage, SR may worsen the throughput performance. To address the problem, PETAL predicts the spectral efficiency when the eNB performs SR and when it does not and compares them. After that, PETAL performs SR only if the spectral efficiency of SR is expected to be higher than the case of non-SR. PETAL leverages CQI reports from UE and the average wait-time duration for the spectral efficiency estimation.

4.4.1 CQI Management

PETAL collects CQI reports for each UE because each UE can be in the different environment (e.g., distance from the eNB, distance from interferers, the number of interferers, etc.). To adapt quickly to the environmental change, PETAL only consider the most recent 200 CQIs. Furthermore, PETAL collects separately CQI reports from subframes which is transmitted with maximum transmission power (non-SR CQI reports) and subframes which is transmitted with reduced transmission power (SR CQI reports).

4.4.2 Success Probability and Airtime Ratio Estimation

PETAL utilizes the distribution of past CQI reports to calculate the success probability of specific MCS index. For success probability estimation of the non-SR case, PETAL leverages CQI reports from subframes which is transmitted without SR in the past. Success probability of MCS which corresponds to CQI q can be calculated as follows:

$$p_{\mathrm{nonSR},q} = \frac{\sum_{i=q}^{15} N_i}{\sum_{i=0}^{15} N_i}; \tag{4.2}$$

$$p_{\mathrm{SR},q} = \frac{\sum_{i=q}^{15} M_i}{\sum_{i=0}^{15} M_i}, \tag{4.3}$$

where N_i and M_i are the number of CQI reports whose value is i among non-SR CQI reports and SR CQI reports, respectively. If there is no SR CQI reports PETAL utilizes CQI reports which are affected by collision interference among non-SR CQI reports

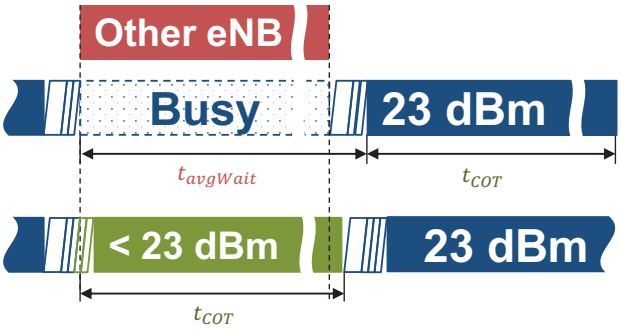

Figure 4.6: Spectral efficiency estimation of PETAL.

as follows:

$$p_{\mathrm{SR},q} = \frac{\sum_{i=q}^{c} N_i}{\sum_{i=0}^{c} N_i}, \tag{4.4}$$

where c is the maximum CQI value among CQI reports which are in the collision cluster of non-SR CQI reports.

On the other hand, PETAL calculates the airtime ratio to estimate spectral efficiency when PETAL does not operate SR. The airtime ratio can be calculated as follows:

$$r_{\mathrm{air}} = \frac{t_{\mathrm{COT}}}{t_{\mathrm{COT}} + t_{\mathrm{avgWait}}}, \tag{4.5}$$

where t_{COT} and t_{avgWait} are time duration of the next COT and the duration of average waiting time (i.e., the time gap between the timing when PETAL decides not to operate SR and the transmission start timing in the past). PETAL leverages an exponentially weighted moving average (EWMA) for t_{avgWait} tracking as follows:

$$t_{\mathrm{avgWait}} = \alpha \cdot t_{\mathrm{avgWait,past}} + (1 - \alpha) \cdot t_{\mathrm{wait}}, \tag{4.6}$$

where α, $t_{\mathrm{avgWait,past}}$, and t_{wait} are the weighting coefficient, the past average waiting time, and the newly measured waiting time. We use 0.75 for the above weighting coefficient α in this chapter.

Table 4.1: Simulation settings for Chapter 4 evaluation.

Simulation settings	Value
Simulation time	5 s
Number of iterations	10
File size	0.5 MB
Bandwidth	20 MHz
eNB transmission power	23 dBm
UE transmission power	23 dBm
Default LAA CCA-ED threshold	-72 dBm

4.4.3 CQI Clustering Algorithm

4.4.4 SR Decision

If PETAL observes the signal, which has energy level between -72 dBm and -62 dBm, in the middle of its backoff procedure, PETAL estimates the spectral efficiency values for non-SR operation and SR operation as follows:

$$SE_{\mathrm{nonSR}} = \max_{0 \le j \le 15} (SE_j \times p_{\mathrm{nonSR},j} \times r_{\mathrm{air}}); \tag{4.7}$$

$$SE_{\mathrm{SR}} = \begin{cases} \max_{0 \le j \le 15}(SE_j \times p_{\mathrm{SR},j}), & \text{if there are SR CQI reports;} \\ \max_{0 \le j \le c}(SE_j \times p_{\mathrm{SR},j}), & \text{otherwise.} \end{cases} \tag{4.8}$$

If there is no SR CQI reports and no collision cluster, PETAL operates SR because it means that there is no impact of interference. In the other cases, PETAL operates SR only if SE_{SR} is greater than SE_{nonSR}.

4.5 Performance Evaluation

We evaluate the performance of PETAL via *ns-3* simulation. We have implemented an coexistence model between LAA and Wi-Fi in *ns-3.22* [27], where LTE and Wi-Fi

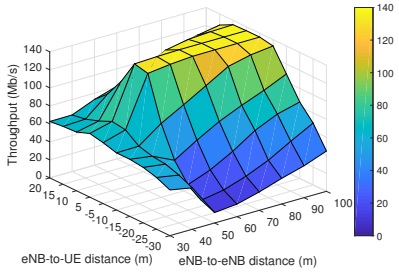

(a) Throughput performance of baseline algorithm.

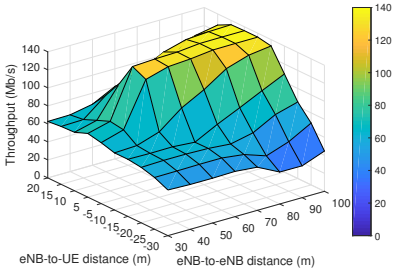

(b) Throughput performance of PETAL.

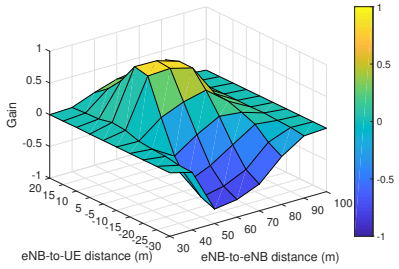

(c) Gain of baseline algorithm.

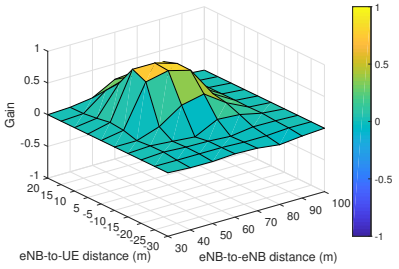

(d) Gain of PETAL.

Figure 4.7: Throughput performance of baseline algorithm and PETAL.

models are implemented separately in the original version. In particular, following features have been implemented: Interference between LAA and Wi-Fi, multiple-input multiple-output (MIMO) for LAA and Wi-Fi, LBT, reservation signal, initial and ending partial subframe, 3GPP indoor hotspot channel model, and 3GPP file transfer protocol (FTP) traffic model [3]. In 3GPP FTP model, 0.5 MB files arrive according to a Poisson process. User datagram protocol (UDP) is used for file transmission. We make all transmitters have saturated traffic. The detailed simulation settings are summarized in Table 4.1.

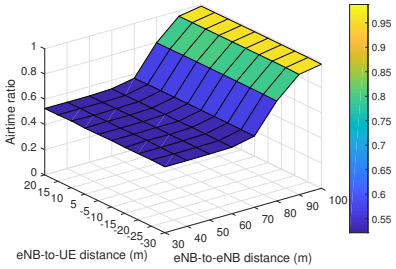

(a) Standard LAA.

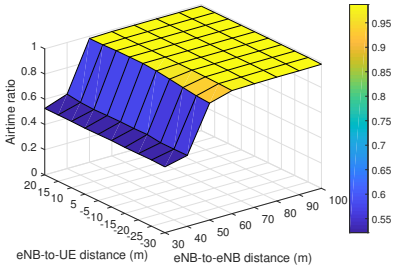

(b) Baseline algorithm.

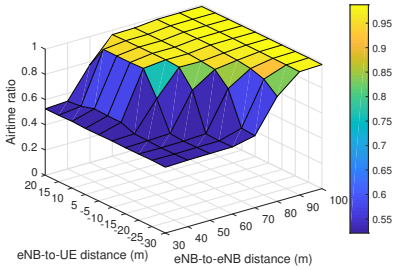

(c) PETAL.

Figure 4.8: Airtime usage.

4.5.1 Two Cell Scenario

We evaluate PETAL in a scenario where two pairs of a single eNB and a UE as illustrated in Fig. 4.2. As we discussed in Section 4.3, the baseline algorithm degrades throughput performance severely when the UE is close to the interferer. Fig. 4.7 shows the throughput performance and the gain over standard LAA of the baseline algorithm and PETAL. We can see that PETAL does not degrade throughput performance even if the UE is close to the interferer (i.e., the other eNB in this case) in Fig. 4.7d. At the same time, PETAL achieves throughput gain as much as the baseline algorithm does when the UE is far from the interferer.

This is because PETAL does not operate SR when SR operation will get much less spectral efficiency than non-SR operation. In Fig. 4.8, we can see that the baseline algorithm operates SR aggressively and utilizes full airtime when the eNB-to-eNB

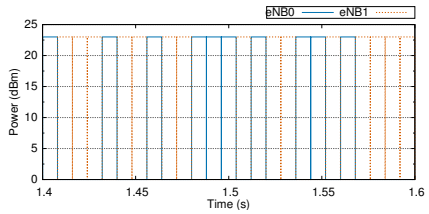

(a) Power usage of standard LAA (0.2 s).

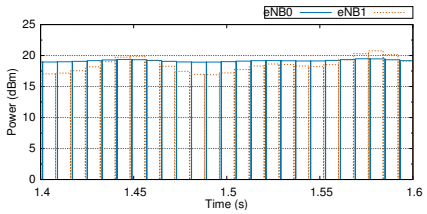

(b) Power usage of PETAL (0.2 s).

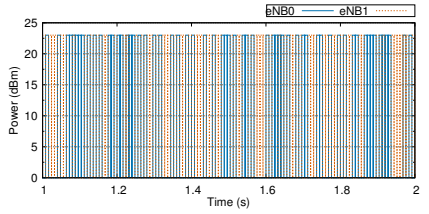

(c) Power usage of standard LAA (1 s).

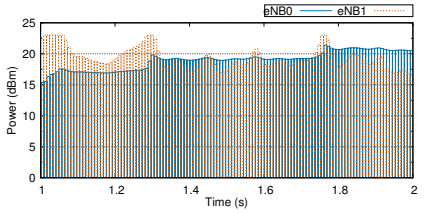

(d) Power usage of PETAL (1 s).

Figure 4.9: Power usage.

distance is between 50 m and 80 m. However, PETAL does not operate SR and use less airtime when PETAL determines that spectral efficiency will be degraded with SR operation.

Fig. 4.9 illustrates the behavior of standard LAA and PETAL in this two cell scenario where the eNB-to-eNB distance and the eNB-to-UE distance are 50 m and 5 m, respectively. The solid line and dotted line represent the transmission power of eNB0 and eNB1, respectively. Figs. 4.9a and 4.9c shows used transmission power of standard LAA while Figs. 4.9b and 4.9d shows used transmission power of PETAL. Standard LAA eNBs use fixed transmission power and only one eNB utilizes channel except when there is a stochastic collision. On the other hand, PETAL eNBs reduce its own transmission power (and increase energy detection threshold accordingly) and enjoy simultaneous transmission (i.e., SR).

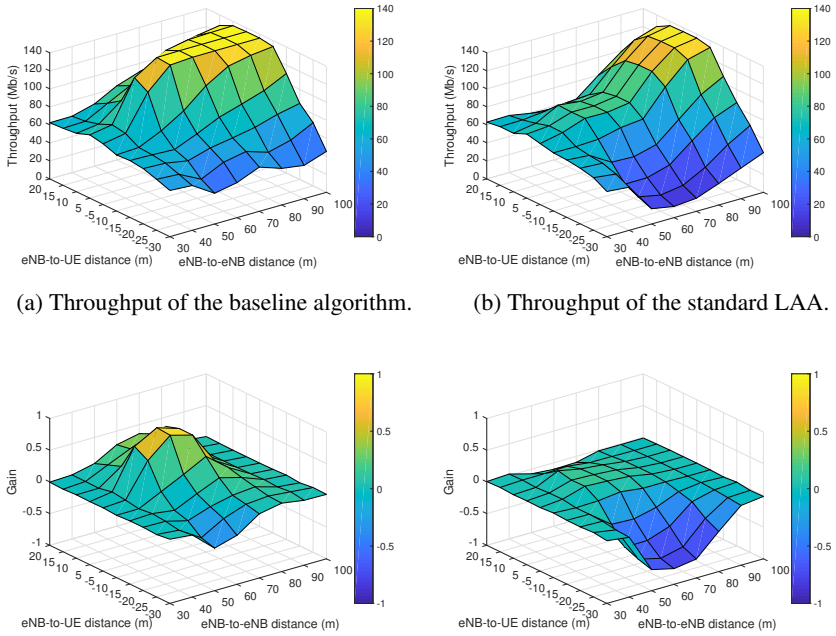

(a) Throughput of the baseline algorithm.

(b) Throughput of the standard LAA.

(c) Gain of the baseline algorithm.

(d) Gain of the standard LAA.

Figure 4.10: Coexistence of the baseline algorithm and standard LAA.

4.5.2 Coexistence with Standard LAA

Figs. 4.10 and 4.11 shows the throughput performance when the standard LAA coexists with the baseline algorithm and PETAL, respectively. In the baseline algorithm and the standard LAA coexistence case, when the UE is close to the other eNB, the throughput gain of the eNB using the baseline algorithm is slightly less than zero, while the throughput gain of the standard LAA eNB is much lower than that. This is because of the fact that the eNB using the baseline algorithm can utilize much more airtime than the coexisting standard LAA eNB.

On the other hand, the eNB using PETAL does not operate SR when SR operation can bring the throughput degradation and the throughput gain is over zero in every situation as we can see in Fig. 4.11c.

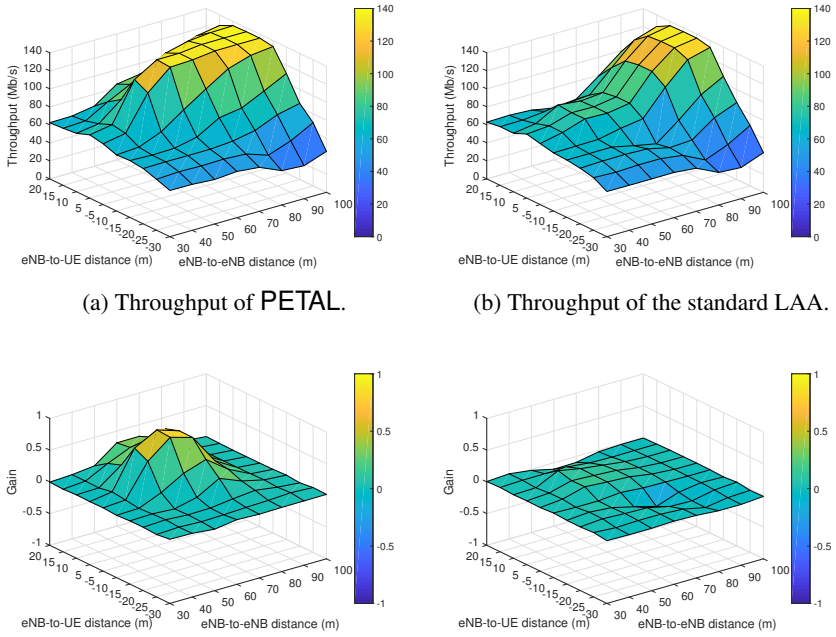

(a) Throughput of PETAL.

(b) Throughput of the standard LAA.

(c) Gain of PETAL.

(d) Gain of the standard LAA.

Figure 4.11: Coexistence of PETAL and standard LAA.

4.5.3 Four Cell Scenario

We also evaluate PETAL in the scenario where four pairs of an eNB and a UE coexist. As illustrated in Fig. 4.12, eNBs are deployed 20 m apart from each other and UEs are deployed randomly in the 50×100 m^2 area. Fig. 4.13 shows the CDF of per UE throughput performance of PETAL in 50 different random topologies. In this scenario, the baseline algorithm, which operates SR most aggressively, shows lower throughput performance than the standard LAA for the bottom 85% cases, while it shows higher throughput performance than the standard LAA in the remaining cases. Fig. 4.13 illustrates the throughput performance of PETAL follows the most outer curve because PETAL suppresses SR operation when the target UE will severely suffer from concurrent interference.

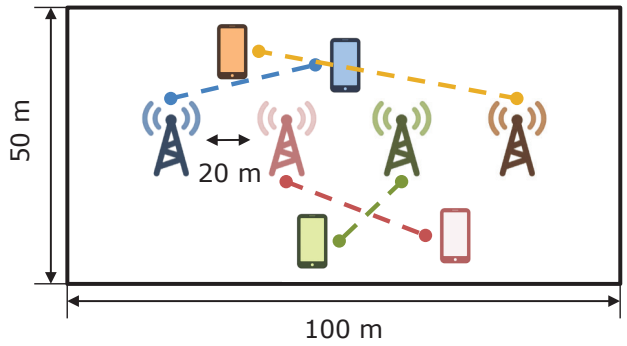

Figure 4.12: Sample of random topologies for 4 cell scenario.

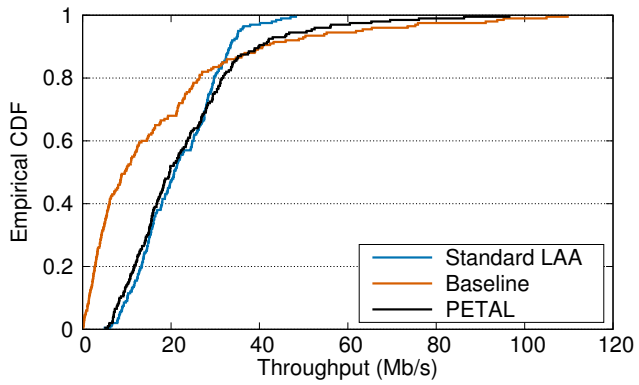

Figure 4.13: Multiple eNBs scenario: Four pairs of an eNB and a UE.

4.6 Summary

In this chapter, we have proposed PETAL to mitigate the negative impact of SR operation. We first design the baseline algorithm, which operates SR aggressively, and show that the baseline algorithm degrades the throughput performance severely when the UE is close to an interferer. Our proposed algorithm PETAL estimates and compares the spectral efficiency for the SR operation and non-SR operation. Then, PETAL operates SR only if the spectral efficiency of SR operation is expected to be higher than the case of non-SR operation. Our simulation verifies the performance of PETAL in various scenarios. When two pair of an eNB and a UE coexists, PETAL improves

the throughput by up to 329% over the baseline algorithm.

Chapter 5

Concluding Remarks

5.1 Research Contributions

In this dissertation, we have addressed the performance enhancement schemes in LAA.

In Chapter 2, we investigate the airtime fairness in various scenarios and show that Wi-Fi's airtime can be less than the coexisting LAA's airtime especially with saturated traffic. To solve the problem, we have proposed RACOTA, a standard compliant COT adaptation algorithm. Through extensive system level simulations, we verify that RACOTA can provide a fair amount of airtime to the coexisting Wi-Fi network.

In Chapter 3, we identify that the conventional link adaptation scheme, i.e., AMC, can choose the wrong MCS due to collision interference in the unlicensed spectrum. Our proposed algorithm COALA utilizes CQI reports and k-means clustering algorithm to mitigate the detrimental effect of intermittent interference on LAA's MCS selection. Through extensive system level simulations, we verify that COALA can improve throughput performance in various scenarios.

In Chapter 4, we show that spatial reuse should not be used if the simultaneous transmission will introduce significant interference to the UE. Our proposed algorithm PETAL decides wisely whether to operate SR or not, based on spectral efficiency estimation. Through extensive system level simulations, we verify that PETAL performs a

spatial reuse operation only in cases where the spatial reuse operation of the baseline algorithm improves the throughput performance.

Bibliography

[1] Recommendation ITU-R M.2083-0, *IMT Vision – Framework and overall objectives of the future development of IMT for 2020 and beyond*, Sept. 2015.

[2] 3GPP TS 36.213 v14.4.0, *Evolved universal terrestrial radio access (E-UTRA) Physical layer procedures (Release 14)*, Sept. 2017.

[3] 3GPP TR 36.889 v13.0.0, *Study on licensed-assisted access to unlicensed spectrum (Release 13)*, June 2015.

[4] N. Rupasinghe and I. Güvenç, "Licensed-assisted access for WiFi-LTE coexistence in the unlicensed spectrum," in *Proc. IEEE GLOBECOM Workshop*, 2014, pp. 894–899.

[5] J. Jeon, Q. C. Li, H. Niu, A. Papathanassiou, and G. Wu, "LTE in the unlicensed spectrum: A novel coexistence analysis with WLAN systems," in *Proc. IEEE GLOBECOM*, 2014, pp. 3459–3464.

[6] Y. Jian, C.-F. Shih, B. Krishnaswamy, and R. Sivakumar, "Coexistence of Wi-Fi and laa-lte: Experimental evaluation, analysis and insights," in *Proc. IEEE ICC Workshop*, 2015, pp. 2325–2331.

[7] Z. Guan and T. Melodia, "CU-LTE: Spectrally-efficient and fair coexistence between LTE and Wi-Fi in unlicensed bands," in *Proc. IEEE INFOCOM*, 2016.

[8] C. Cano and D. J. Leith, "Coexistence of wifi and LTE in unlicensed bands: A proportional fair allocation scheme," in *Proc. IEEE ICC Workshop*, 2015, pp. 2288–2293.

[9] A. K. Sadek, T. Kadous, K. Tang, H. Lee, and M. Fan, "Extending LTE to unlicensed band-merit and coexistence," in *Proc. IEEE ICC Workshop*, 2015, pp. 2344–2349.

[10] W. J. Hillery, N. Mangalvedhe, R. Bartlett, Z. Huang, and I. Z. Kovacs, "A network performance study of LTE in unlicensed spectrum," in *Proc. IEEE GLOBECOM Workshop*, 2015, pp. 1–7.

[11] S. Sagari, S. Baysting, D. Saha, I. Seskar, W. Trappe, and D. Raychaudhuri, "Coordinated dynamic spectrum management of lte-u and Wi-Fi networks," in *Proc. IEEE DySPAN*, 2015, pp. 209–220.

[12] J. Xiao and J. Zheng, "An adaptive channel access mechanism for lte-u and wifi coexistence in an unlicensed spectrum," in *Proc. IEEE ICC*, 2016, pp. 1–6.

[13] V. Maglogiannis, D. Naudts, A. Shahid, and I. Moerman, "A q-learning scheme for fair coexistence between LTE and Wi-Fi in unlicensed spectrum," vol. 6, pp. 27 278–27 293, 2018.

[14] S. Dama, A. Kumar, and K. Kuchi, "Performance evaluation of laa-lbt based LTE and wlan's co-existence in unlicensed spectrum," in *Proc. IEEE GLOBECOM Workshop*, 2015, pp. 1–6.

[15] J. Jeon, H. Niu, Q. Li, A. Papathanassiou, and G. Wu, "LTE with listen-before-talk in unlicensed spectrum," in *Proc. IEEE ICC Workshop*, 2015, pp. 2320–2324.

[16] A. M. Voicu, L. Simić, and M. Petrova, "Coexistence of pico-and femto-cellular lte-unlicensed with legacy indoor Wi-Fi deployments," in *Proc. IEEE ICC Workshop*, 2015, pp. 2294–2300.

[17] A. Mukherjee *et al.*, "Licensed-assisted access LTE: Coexistence with ieee 802.11 and the evolution toward 5G," *IEEE Commun. Mag.*, vol. 54, no. 6, pp. 50–57, 2016.

[18] R. Yin, G. Yu, A. Maaref, and G. Y. Li, "Adaptive lbt for licensed assisted access LTE networks," in *Proc. IEEE GLOBECOM*, 2015, pp. 1–6.

[19] Y. Li, T. Zhou, Y. Yang, H. Hu, and M. Hamalainen, "Fair downlink traffic management for hybrid LAA-LTE/Wi-Fi networks," vol. 5, pp. 7031–7041, 2017.

[20] C. Hasan, M. K. Marina, and U. Challita, "On LTE-WiFi coexistence and inter-operator spectrum sharing in unlicensed bands: Altruism, cooperation and fairness," in *Proc. ACM MobiHoc*, 2016, pp. 111–120.

[21] ETSI, "301 893 broadband radio access networks (BRAN); 5 GHz high performance RLAN; harmonized EN covering the essential requirements of article 3.2 of the R&TTE directive," vol. 2.1.1, 2017.

[22] B. Jia and M. Tao, "A channel sensing based design for LTE in unlicensed bands," in *Proc. IEEE ICC Workshop*, 2015, pp. 2332–2337.

[23] M. Mehrnoush and S. Roy, "On the fairness of Wi-Fi and LTE-LAA coexistence," *arXiv preprint arXiv:1805.03501*, 2018.

[24] E. Chai, K. Sundaresan, M. A. Khojastepour, and S. Rangarajan, "LTE in unlicensed spectrum: Are we there yet?" in *Proc. ACM MobiCom*, 2016, pp. 135–148.

[25] IEEE 802.11-2012, *Part 11: Wireless LAN medium access control (MAC) and physical layer (PHY) specifications*, IEEE Std., Mar. 2012.

[26] IEEE 802.11ac, *Part 11: Wireless LAN medium access control (MAC) and physical layer (PHY) specifications: Enhancements for very high throughput for operation in bands below 6 GHz*, IEEE Std., Dec. 2013.

[27] ns 3 project, ns-3 manual, Release ns-3.22. (2015, Feb. 26). [Online]. Available: https://www.nsnam.org/documentation/.

[28] 3GPP TR 36.814 v9.0.0, *Evolved universal terrestrial radio access (E-UTRA) further advancements for E-UTRA physical layer aspects (Release 9)*, Mar. 2010.

[29] Y. Li, G. Drory, Y. Cohen, B. Yang, M. Fischer, S. Levy, S. Verma, and S. Adhikari, "WiFi-coordinated LAA-LTE," U.S. Patent 20 160 095 110, Mar. 31, 2016.

[30] Ath9k: Atheros linux wireless driver. [Online]. Available: http://wireless.kernel.org/en/users/Drivers/ath9k/.

[31] HostAP: IEEE 802.11 AP, IEEE 802.1X/WPA/WPA2/EAP/RADIUS authenticator. [Online]. Available: http://hostap.epitest.fi/hostapd/.

[32] Iperf: The TCP/UDP Bandwidth Measurement Tool. [Online]. Available: http://dast.nlanr.net/Projects/Iperf/.

[33] K. Yoon, T. Park, J. Kim, W. Sun, S. Hwang, I. Kang, and S. Choi, "COTA: Channel occupancy time adaptation for LTE in unlicensed spectrum," in *Proc. IEEE DySPAN*, 2017, pp. 181–190.

[34] S. Ahmadi, *LTE-Advanced: A practical systems approach to understanding 3GPP LTE releases 10 and 11 radio access technologies*. Academic Press, 2013.

[35] S. Sesia, M. Baker, and I. Toufik, *LTE - The UMTS long term evolution: From theory to practice*. John Wiley & Sons, 2011.

[36] G. Ku and J. M. Walsh, "Resource allocation and link adaptation in LTE and LTE Advanced: A tutorial," *IEEE Commun. Surv. Tuts.*, vol. 17, no. 3, pp. 1605–1633, 2015.

[37] 3GPP TS 36.211 v14.4.0, *Evolved universal terrestrial radio access (E-UTRA) Physical channels and modulation (Release 14)*, Sept. 2017.

[38] X. Yan, H. Tian, C. Qin, and A. Paulraj, "Constrained stochastic game in licensed-assisted access for dynamic contention window adaptation," *IEEE Commun. Lett.*, 2017.

[39] Q. Zhang, Q. Wang, Z. Feng, and T. Yang, "Design and performance analysis of a fairness-based license-assisted access and resource scheduling scheme," *IEEE J. Sel. Areas Commun.*, vol. 34, no. 11, pp. 2968–2980, 2016.

[40] A. Galanopoulos, F. Foukalas, and T. A. Tsiftsis, "Efficient coexistence of LTE with wifi in the licensed and unlicensed spectrum aggregation," *IEEE Trans. Cogn. Commun. Netw.*, vol. 2, no. 2, pp. 129–140, 2016.

[41] K. Yoon *et al.*, "COTA: Channel occupancy time adaptation for LTE in unlicensed spectrum," in *Proc. IEEE DySPAN*, 2017, pp. 1–10.

[42] A. Bhorkar, C. Ibars, A. Papathanassiou, and P. Zong, "Medium access design for LTE in unlicensed band," in *Proc. IEEE WCNCW*, 2015, pp. 369–373.

[43] S. Lloyd, "Least squares quantization in PCM," *IEEE Trans. Inform. Theory*, vol. 28, no. 2, pp. 129–137, 1982.

[44] R. Tibshirani, G. Walther, and T. Hastie, "Estimating the number of clusters in a data set via the gap statistic," *J. R. Stat. Soc. Ser. B-Stat. Methodol.*, vol. 63, no. 2, pp. 411–423, 2001.

[45] J. A. Hartigan and M. A. Wong, "Algorithm as 136: A *k*-means clustering algorithm," *J. R. Stat. Soc. Ser. C-Appl. Stat.*, vol. 28, no. 1, pp. 100–108, 1979.

[46] D. M. Christopher, R. Prabhakar, and S. Hinrich, "Introduction to information retrieval," *An Introduction To Information Retrieval*, vol. 151, p. 177, 2008.

[47] J. Li, X. Wang, D. Feng, M. Sheng, and T. Q. Quek, "Share in the commons: Coexistence between lte unlicensed and wi-fi," *IEEE Wireless Commun. Mag.*, vol. 23, no. 6, pp. 16–23, 2016.

[48] L. Falconetti, R. Karaki, E. Obregon, J.-F. Cheng, H. Koorapaty, A. Mukherjee, S. Falahati, D. Larsson *et al.*, "Design and evaluation of licensed assisted access lte in unlicensed spectrum," *IEEE Wireless Commun. Mag.*, vol. 23, no. 6, pp. 24–30, 2016.

[49] Y. Li, J. Zheng, and Q. Li, "Enhanced listen-before-talk scheme for frequency reuse of licensed-assisted access using lte," in *Proc. IEEE International Symposium on Personal, Indoor and Mobile Radio Communications (PIMRC)*. IEEE, 2015, pp. 1918–1923.

초 록

비면허 대역에서의 LTE 동작은 더 높은 데이터 전송률을 달성하는 유망한 기술로 부각되고 있다. 최근 3GPP는 기존 Wi-Fi 기술이 사용하던 5 GHz 비면허 대역에서 LTE를 사용하는 licensed-assisted access (LAA) 기술의 표준화를 완료하였다.

본 논문에서 우리는 LAA의 성능을 향상시키기 위해 다음과 같은 세 가지 전략을 제안한다: (1) 수신기 인식 채널 점유 시간 적응, (2) 충돌 인식 링크 적응, (3) 전력 및 에너지 검출 역치 적응.

첫째, LAA는 고정된 최대 채널 점유 시간을 가지고 있고 그 시간 만큼 연속적으로 전송할 수 있는 반면, Wi-Fi는 비교적 짧은 시간 동안만 연속적으로 전송할 수 있다. 그 결과 Wi-Fi가 LAA와 공존할 때 Wi-Fi의 airtime과 수율 성능은 Wi-Fi가 또 다른 Wi-Fi와 공존할 때에 비하여 저하되게된다. 따라서 우리는 Wi-Fi의 airtime과 수율 성능을 향상시키기 위하여 Wi-Fi의 A-MPDU 프레임 전송 시간에 맞추어 LAA의 채널 점유 시간을 조절하는 수신기 인식 채널 점유 시간 적응 기법인 RACOTA를 제안한다. RACOTA는 포화 감지 결과 Wi-Fi 수신기가 더 받을 데이터가 있다고 판단될 때에만 채널 점유 시간을 조절한다. 우리는 RACOTA의 포화 감지 알고리즘을 상용 Wi-Fi 장비에 구현하여 이를 바탕으로 실측을 통해 RACOTA가 공존하는 Wi-Fi의 포화 여부를 정확하게 감지해냄을 보인다. 또한 우리는 ns-3 시뮬레이션을 통하여 RACOTA를 사용하는 LAA가 공존하는 Wi-Fi에게 공정한 airtime을 제공하고 기존 LAA와 공존하는 Wi-Fi 대비 최대 334%의 Wi-Fi 수율 성능 향상을 가져옴을 보인다.

둘째, 간헐적인 충돌이 발생할 수 있는 비면허 대역에서는 기존 LTE의 링크 적

응 기법인 adaptive modulation and coding (AMC)이 잘 동작하지 않을 수 있다. 간헐적인 충돌은 LAA 기지국으로 하여금 modulation and coding scheme (MCS)을 낮추어서 다음 전송을 하도록 하는데 다음 전송 시에 충돌이 발생하지 않는다면 불필요하게 낮춘 MCS로 인해 주파수 효율이 크게 저하된다. 이러한 문제를 해결하기 위해 우리는 충돌 인식 링크 적응 기법인 COALA를 제안한다. COALA는 k-means 무감독 클러스터링 알고리즘을 사용하여 channel quality indicator (CQI) 리포트 중 충돌 간섭에 영향을 받은 CQI 리포트들을 구별해내고 이를 통해 다음 전송을 위한 최적의 MCS를 선택한다. 우리는 실측을 통하여 COALA가 정확하게 충돌을 감지해냄을 보인다. 또한 우리는 다양한 환경에서의 ns-3 시뮬레이션을 통하여 COALA가 AMC 대비 최대 74.9%의 사용자 인식 수율 성능 향상을 가져옴을 보인다.

셋째, 우리는 공간 재사용 동작의 부작용을 최소화하기 위하여 수신 단말을 고려하여 전송 파워 및 에너지 검출 역치를 적응적으로 조절하는 PETAL 알고리즘을 제안한다. 우리는 먼저 수신 단말을 고려하지 않고 공격적으로 공간 재사용 동작을 하는 baseline 알고리즘을 설계하고 다양한 환경에서의 시뮬레이션을 통하여 수신 단말이 간섭원에 가까운 경우 baseline 알고리즘의 성능이 심각하게 열화됨을 보인다. 제안하는 알고리즘인 PETAL은 수신 단말로부터 받은 CQI 리포트 정보와 채널 점유 시점까지의 평균 대기 시간을 이용하여 공간 재사용 동작을 할 때 예상되는 주파수 효율과 공간 재사용 동작을 하지 않을 때 예상되는 주파수 효율을 비교하여 공간 재사용 동작을 할 때 예상되는 주파수 효율이 더 클 때에만 공간 재사용 동작을 한다. 우리는 다양한 환경에서의 ns-3 시뮬레이션을 통하여 PETAL이 baseline 알고리즘 대비 최대 329%의 수율 성능 향상을 가져옴을 보인다.

요약하자면, 우리는 LAA의 등장과 함께 새롭게 대두되는 흥미로운 문제들을 확인하고 문제들의 심각성을 다양한 환경에서의 시뮬레이션을 통하여 살펴보고 이러한 문제들을 해결할 수 있는 알고리즘들을 제안한다. Wi-Fi와 LAA 사이의 airtime 공정성은 LAA의 연속 전송 시간을 적응적으로 조절하여 개선할 수 있다. 또한 링크 적응 정확도와 공간 재사용 동작의 효율성은 CQI 리포트들의 분포를 이용하여 개선할 수 있다. 제안하는 알고리즘들의 성능은 시스템 레벨 시뮬레이션을 통하여 검증되었다.

주요어: Airtime 공정성, licensed-assisted access (LAA), 링크 적응, 파워 조절, 공간 재사용.
학번: 2012-20816

감사의 글

멀티미디어 무선통신망 연구실은 저에게 인큐베이터와 같은 곳이었습니다. 통신에 관심을 갖고 인턴을 시작했을 때부터 졸업을 앞둔 지금까지 연구실에서 너무도 많은 것을 배웠습니다. 존경하는 지도교수님과 뛰어난 선후배들의 지도와 도움이 있었기에 이 학위논문을 포함한 그간의 연구 성과들을 발표할 수 있었습니다. 저의 석사박사통합과정 중 다방면으로 도움을 주신 모든 분들께 이 자리를 빌어 감사의 말씀을 전합니다.

부족한 점이 많은 저를 오랜 시간 희생과 헌신으로 지도해주신 최성현 지도교수님께 진심으로 깊은 감사를 드립니다. 제 인생에 있어 최성현 교수님을 만난 것은 너무나 큰 축복이라고 생각합니다. 깊은 통찰력과 넓은 학문적 스펙트럼을 가지신 교수님과 함께 연구하면서 저의 게으른 연구 자세를 깨닫고 반성할 수 있었습니다. 또한 현실적인 문제에 집중하여 해결하는 태도와 어려움이 있어도 끈질기게 매달리는 태도를 기를 수 있었습니다. 무엇보다도 교수님의 리더쉽에 큰 감명을 받았습니다. 꽤 규모가 큰 연구실임에도 모두가 교수님을 존경하며 서로 도와주는 문화가 형성되어 있는 것은 입학할 당시부터 제게 큰 놀라움이었습니다. 아직도 최성현 교수님의 리더쉽의 비밀을 다 배우지 못하였지만 졸업 후에도 계속 옆에서 보고 배우겠습니다.

학위논문의 심사위원이신 박세웅 교수님, 임종한 교수님, 김성륜 교수님, 윤지훈 교수님께도 깊은 감사의 말씀을 드립니다. 연례 공동 워크샵을 통하여 귀한 지도해주신 박세웅 교수님께 감사의 말씀을 드립니다. 학부 시절 박세웅 교수님과 성경공부를 했던 추억과 네트워크 연구실을 성경 말씀대로 이끌어가시는 박세웅 교수님의

모습은 졸업 후 시간이 많이 흘러도 잊지 못할 것 같습니다. 짧은 시간이지만 매주 세미나를 통하여 큰 가르침을 주신 임종한 교수님께 감사의 말씀을 드립니다. 비록 제가 속한 LAA 팀과의 교류는 많지 않았지만 여러 기회로 발표할 때 마다 귀중한 조언을 주셔서 많이 배울 수 있었습니다. RRC 연구 과제의 총괄 책임자로서 연구단의 연구 방향을 지도해주시고 제 연구에도 큰 관심으로 도움을 주신 김성륜 교수님께 감사의 말씀을 드립니다. 김성륜 교수님께서 RRC 연구 과제의 방향을 잘 이끌어주셨기 때문에 이 학위논문에 포함된 연구 성과들이 나올 수 있었습니다. 제 연구에 큰 관심을 가져주시고 깊은 통찰력으로 많은 지도를 해주신 윤지훈 교수님께 감사 말씀을 드립니다. 윤지훈 교수님의 LAA 관련 강연들을 통해 많은 것을 배울 수 있었습니다.

석사 시절 많은 가르침을 주시고 이후에도 연구 및 진로에 있어서 조언을 아끼지 않으신 류봉균 박사님께도 깊은 감사의 말씀을 드리며 EpiSys의 무궁한 발전을 위해 기도합니다. 짧은 만남이었지만 귀한 조언으로 연구에 도움을 주신 김효일 교수님께도 감사의 말씀을 드립니다.

소중한 멀티미디어 무선통신망 연구실 선후배님들에게도 감사의 말씀을 드립니다. 비록 연구실에서 함께하지는 못했지만 먼저 사회에 진출하셔서 연구실의 앞길을 밝혀주신 선배님들께 감사의 말씀을 전합니다. 통신에 대해 아무것도 모르는 시절 귀찮은 내색없이 알려주시고 도와주신 최문환, Edwin, 이혜원, 이원보, 이옥환, 조병갑, 곽규환, Ildefonso 선배님들께 감사의 말씀을 전합니다. 연구실 출신 1호 창업자로써 귀한 경험을 공유해주시고 연구와 창업의 유사성을 알려주신 김태현 선배님에게 감사드립니다. 연구실의 고년차로써 저를 포함한 후배들을 잘 이끌어준 홍종우, 유승민, 곽규환 선배님들께 감사의 인사를 드립니다. 연구실에서 오랫동안 함께하며 선배로써 친구로써 많은 추억을 쌓은 신연철, 구종회, 김성원, 변성호, 박승일에게 고마운 마음을 전합니다. 2년동안 함께하였고 많은 짐을 대신 지어주었던 동기 서지훈에게도 고맙다는 말을 남깁니다. LAA 연구를 함께하며 동고동락했던 손위평, 박태준, 김지훈, 이재홍, 황선욱에게도 고마운 마음 전합니다. 특히 김지훈, 이재홍, 황선욱에게는 더 좋은 선배가 되어주지 못해서 미안하다는 말을 남기고 싶습니다. 남은 박사과정 기간 동안 많은 연구 성과 이루며 즐겁게 생활하기를 기

도합니다. 뉴미연에서 함께 연구하며 추억을 쌓은 김선도, 김준석, 윤호영, 이기택, 허재원, 장민석, 김병준, 임수훈, 302동의 이규진, 양창목, 손영욱, 최준영, 곽철영, 이지환, 가순원, 이주헌, 이강현, 권휘재, 이경진에게도 감사와 격려의 인사를 남깁니다.

비록 같은 연구실은 아니었지만 연구적, 생활적으로 많은 도움을 주신 네트워크 연구실의 윤성국 형님, 김형신, 한종훈, 이태섭, 이현중, 통신 및 신호처리 연구실의 김선욱, 강재열, 박민수, 백승규, 허정륜에게도 감사의 마음을 전합니다.

학부 시절 함께 믿음을 키워나간 IVF 선후배들에게 감사의 말씀을 전합니다. 인생의 방향과 가치관을 세우는 순간들을 함께한 것은 제게 큰 추억입니다. 특히 저의 동기인 김경일, 김덕구, 이상혁, 자이니진, 유지영, 최늘샘, 김지연, 이진주, 장영진, 최인경에게 감사와 응원의 마음을 전합니다.

Wheel life의 기쁨을 알게해준 네이게이토 형제자매들에게도 감사의 마음을 전합니다. 교제의 도움이 아니었더라면 스트레스만 많이 받고 성과는 없었을 것 입니다. 특별히 저에게 마음을 많이 써주신 이명원 선교사님, 명은애 자매님, 유동윤 형님, 송필량 형님, 강유석 형님께 깊은 감사의 말씀을 드립니다.

오랜 시간 연락하며 힘이 되어준 이은규에게도 고마운 마음을 전하며 쌍둥이와 함께 걸어갈 앞으로의 길을 응원합니다. 기쁜 일이나 슬픈 일이나 한 마음으로 함께 해준 곽민준, 김철원, 김현준, 박상현, 박성준, 박재순, 손종구, 장동엽 대광고등학교 친구들에게도 깊은 감사의 마음을 전합니다.

언제나 젊은 마음으로 열정적으로 일하시는 존경하는 아버지, 사랑과 헌신으로 양육해주신 사랑하는 어머니, 가장 신뢰하는 친구가 되어준 여동생에게 깊은 사랑과 감사의 마음을 전합니다. 고집스럽고 제멋대로이며 미성숙한 저를 받아주시고 키워주신 부모님께 항상 존경하며 사랑한다는 말씀을 드리고 싶습니다. 부족한 저를 가족의 일원으로 받아주시고 항상 사랑해주시는 장인어른, 장모님께도 깊은 사랑과 감사의 말씀을 드립니다. 신뢰하는 친구이자 형님인 김원식, 사랑으로 가족들을 챙기는 이동림 처형, 너무나 귀엽고 사랑스러운 김이현, 미국에서 열심히 공부 중인 멋진 처남 이찬우에게도 감사의 마음을 전합니다.

특별히 제 인생의 동반자 이혜림에게 감사의 마음을 전합니다. 그대 옆에 있었기에 어떤 어려움도 힘들게 느껴지지 않았습니다. 순수하고 진실된 그대를 보며 매일 배웁니다.

사랑하는 아들 윤은재에게도 건강하게 태어나줘서 고맙다는 말을 하고싶습니다. 은재에게 세상이 흥미롭고 따뜻한 곳으로 느껴지기를 축복합니다.

의지할 때마다 마음과 생각을 지키시고 이겨낼 힘과 지혜를 주신 하나님께 찬양합니다. 박사과정을 통하여 하나님의 관심과 사랑을 깊이 느낄 수 있었습니다. 어디에서나 빛과 소금이 되어 영혼을 살리는 삶을 살겠습니다.

지혜 있는 자는 궁창의 빛과 같이 빛날 것이요 많은 사람을 옳은 데로 돌아오게 한 자는 별과 같이 영원토록 빛나리라 (다니엘 12장 3절)

2019년 1월

윤강진 올림